
This manuscript, entitled ***Detrital zircon record of the Sturtian glaciation: Adelaide Superbasin***, is a preprint that has not undergone peer-review. It is a version of the manuscript included within the PhD thesis this work forms part of. It is subject to further revision by co-authors prior to journal submission, reviews by thesis examiners, and the peer review process once submitted to a journal. If accepted once submitted to a journal, the final version of this manuscript will be available via the “published version” link at the top of this webpage. Please feel free to contact the main author; we welcome feedback and queries

Jarred C. Lloyd^{1,2}; Wolfgang V. Preiss^{1,3}; Alan S. Collins¹; Georgina M. Virgo^{2,1}; Morgan L. Blades¹; Sarah E. Gilbert⁴; Kathryn J. Amos²

1. Tectonics and Earth Systems Group, and Mineral Exploration CRC, Department of Earth Sciences, University of Adelaide, Adelaide, SA 5005, Australia
2. Australian School of Petroleum and Energy Resources, University of Adelaide, Adelaide, SA 5005, Australia
3. Department for Energy and Mining, Geological Survey of South Australia, Adelaide, SA 5000, Australia
4. Adelaide Microscopy, University of Adelaide, Adelaide, SA 5005, Australia

Corresponding author email: jarred.lloyd@adelaide.edu.au

1 Detrital zircon record of the *Sturtian glaciation*: Adelaide 2 Superbasin

Jarred C. Lloyd^{1,2}; Wolfgang V. Preiss^{1,3}; Alan S. Collins¹; Georgina M. Virgo^{2,1}; Morgan L. Blades¹; Sarah E. Gilbert⁴; Kathryn J. Amos²

- 3 1. Tectonics and Earth Systems Group, and Mineral Exploration CRC, Department of Earth
4 Sciences, University of Adelaide, Adelaide, SA 5005, Australia
- 5 2. Australian School of Petroleum and Energy Resources, University of Adelaide, Adelaide, SA
6 5005, Australia
- 7 3. Department for Energy and Mining, Geological Survey of South Australia, Adelaide, SA 5000,
8 Australia
- 9 4. Adelaide Microscopy, University of Adelaide, Adelaide, SA 5005, Australia

10 Abstract

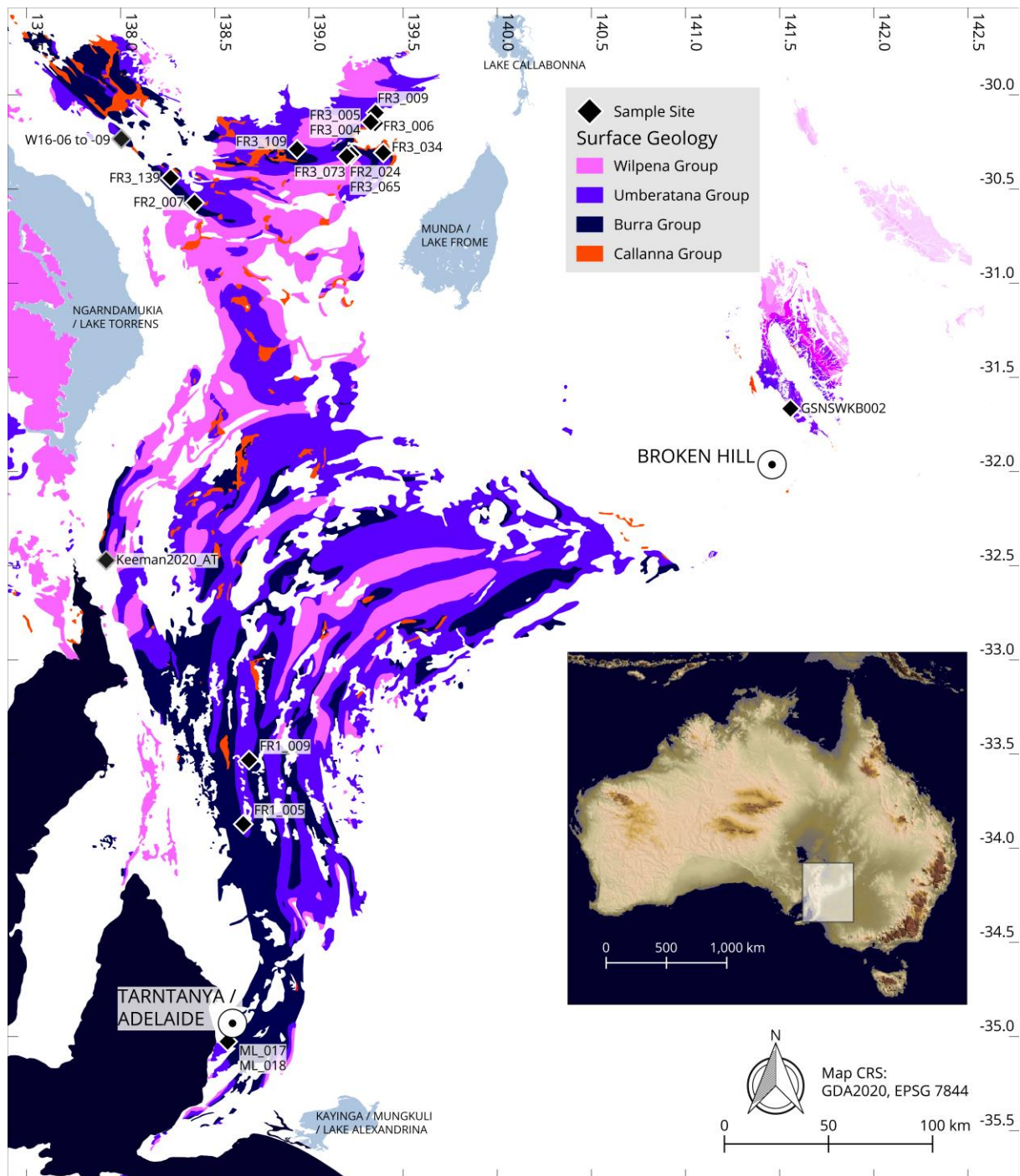
11 The glaciogenic nature of the Yudnamutana Subgroup was first recognised over a
12 century ago, and their global significance was recognised shortly after, eventually
13 culminating with the pan global *Sturtian glaciation* and Snowball Earth theory. Much
14 debate on the origin and timing of these rocks, locally and globally, has ensued in the
15 years since. A significant corpus of research on the lithology, sedimentology,
16 geochronology, and formal stratigraphy of these sequences globally has attempted to
17 resolve many of these debates. In the type area for the *Sturtian glaciation*, South
18 Australia's Adelaide Superbasin, lithostratigraphy and sedimentology have been well
19 understood; however, formal stratigraphy had remained complicated and contested.
20 Geochronology has also been extremely sparse in this area, with limited advancement
21 in the past few years. The result of these longstanding issues has been disagreement as
22 to whether the sedimentary rocks of the Yudnamutana Subgroup are truly correlative
23 throughout South Australia, and if they were deposited in the same time window now
24 defined for and other *Sturtian glacial* rocks globally, c. 717 Ma to c 660 Ma. In this study
25 we present a large detrital zircon study, summarise and compile existing geochronology,
26 and provide an up-to-date understanding of the formal stratigraphy. We confirm that the
27 rocks of the Yudnamutana Subgroup were deposited within the time globally defined for
28 *Sturtian glaciation*.

29 1 Introduction

30 The Neoproterozoic is one of the most pivotal times in Earth's history for earth system
31 changes that led to the Phanerozoic world of extensive macroscopic mineralised life,
32 significantly oxygenated atmosphere and hydrosphere, and a buffered climate devoid of
33 whole-planet glaciations (Halverson et al. 2009; Och & Shields-Zhou 2012; Shields et
34 al. 2022; Tostevin & Mills 2020; Wallace et al. 2017). Within the Neoproterozoic, the
35 Cryogenian Period (derived from the Greek: κρύος, meaning cold), is named for the

36 globally distributed, and long-lasting continental glaciations (Plumb 1991; Plumb &
37 James 1986) characteristic of this time. The record of these glaciations is known on
38 every continent except Antarctica (Arnaud et al. 2011), with notably well studied
39 sections in Australia (Le Heron 2012; Preiss et al. 2011; Virgo et al. 2021), Canada
40 (Hoffman & Halverson 2011; Macdonald et al. 2010; Macdonald et al. 2018), China
41 (Rooney et al. 2020; Wu et al. 2019; Xiao et al. 2020; Xu et al. 2009; Zhang, Q-R et al.
42 2011; Zhu & Wang 2011), Ethiopia (Park et al. 2019), Namibia (Hoffman et al. 2021;
43 Hoffman et al. 2017b; Nascimento et al. 2017), Scotland (Ali et al. 2018; Fairchild et al.
44 2018), Svalbard (Halverson et al. 2017; Halverson et al. 2018), and the USA (Le Heron
45 et al. 2018; Lechte et al. 2018; Link & Christie-Blick 2011; Lund et al. 2011; Mrofka &
46 Kennedy 2011; Petterson et al. 2011). While the concept of a Snowball Earth, and even
47 the glaciogenic nature of these some of these formations remains conjectural to this day
48 (e.g., Allen & Etienne 2008; Eyles & Januszczak 2004; Le Heron et al. 2020; Williams &
49 Gostin 2019), two major glacial episodes are indicated; the older *Sturtian glaciation*,
50 and the younger *Marinoan (Elatina) glaciation* (Hoffman et al. 2017a). These two major
51 glacial events of the Cryogenian have been invoked to be key drivers of nutrient supply
52 into oceans during the interglacial and post-glacial periods and subsequently the rise of
53 algae/eukaryotic life, leading to the emergence of animals (Brocks 2018; Brocks et al.
54 2017; Lechte et al. 2019), key control on carbon enrichment of sediments post-
55 glaciation (Xiao et al. 2020), and as a potential explanation for the Laurentian “Great
56 Unconformity” (Keller et al. 2019).

57 Absolute geochronological constraints have become well established in several of these
58 regions (Rooney et al. 2015) and is ever improving across the globe (e.g. MacLennan et
59 al. 2018; Nascimento et al. 2017; Rud`ko et al. 2020). One notable exception is that of
60 the sequences of Australia where some the thickest and best-preserved Cryogenian
61 glaciogenic formations are found. Until recently (Cox et al. 2018b; Keeman et al. 2020;
62 Lloyd et al. 2020; Rose et al. 2013) radiometric dates of any form for the Cryogenian
63 glaciogenic and interglacial sequences of the Adelaide Superbasin, South Australia,
64 were extremely sparse (Fanning & Link 2006; Ireland et al. 1998; Kendall et al. 2006).
65 This is in part due to the dearth of known volcanogenic horizons within the South
66 Australian Cryogenian sequences, the challenges of dating pre-Cambrian sedimentary
67 rocks (Halverson et al. 2018; Shields et al. 2022), and the general lack of
68 geochronological research conducted on the basin since the marked advancement in
69 laser ablation, and chemical abrasion geochronological techniques during the mid-
70 2000s (Gehrels et al. 2008; Mattinson 2005; Mundil et al. 2004). In this study we
71 address this by presenting 1034 new detrital zircon analyses from fifteen samples
72 [Figure 1] of the Yudnamutana Subgroup (*Sturtian glaciation*), 59 analyses from the
73 thought to be equivalent Yancowinna Subgroup of New South Wales, and an additional
74 56 analyses from the interglacial Serle Conglomerate. The purpose of this paper is not
75 to debate the environmental aspects of this time, but to provide the base of a
76 geochronological framework for the *Sturtian* glaciogenic rocks of the Adelaide
77 Superbasin, i.e., the true *Sturtian*.



78

79

80

Figure 1 – Sample locality map, showing distribution of Neoproterozoic stratigraphy within the Adelaide Rift Complex of the Adelaide Superbasin. GPS coordinates for samples are provided with the U-Pb data (see data availability).

81

2 Geological Background

82

2.1 Adelaide Superbasin

83

The Adelaide Superbasin (Lloyd et al. 2020) is a large, Neoproterozoic to middle

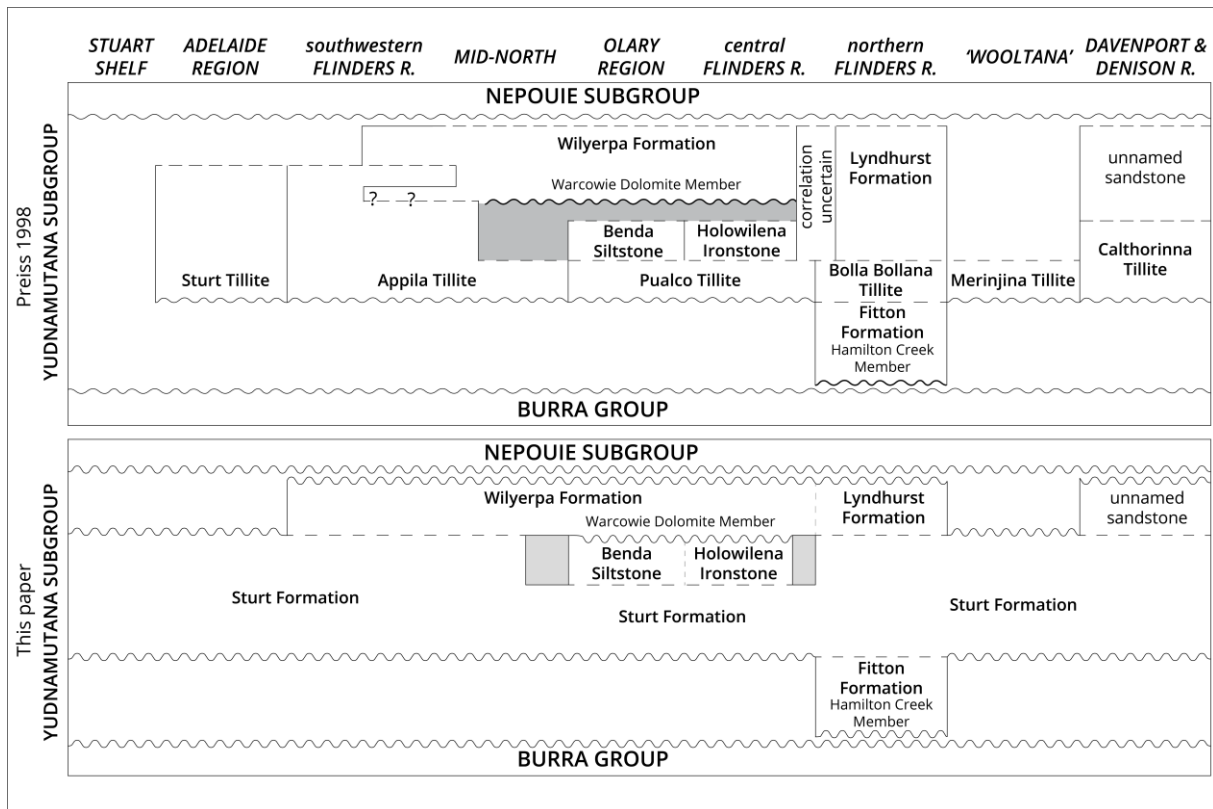
84

Cambrian sedimentary system at the southeast margin of Proterozoic Australia, which

85

formed as a result of the breakup of the supercontinent Rodinia. The Adelaide

86 Superbasin consists of several named basins and sub-basins that span the
87 Neoproterozoic to early Cambrian (Lloyd et al. 2020). The largest and oldest of these is
88 the Adelaide Rift Complex that is contiguous with the relatively undeformed rocks of the
89 Torrens Hinge Zone, Stuart Shelf (Sprigg 1952), and Coombalarnie Platform (Callen
90 1990). Two Cambrian basins, the Arrowie Basin, and the Stansbury Basin, are also
91 considered as part of the Adelaide Superbasin (Lloyd et al. 2020; Preiss et al. 2002).
92 Deposition within the Adelaide Superbasin spans over 300 million years of Earth's
93 history and stretches from the northernmost regions of South Australia, narrowing in the
94 South Mount Lofty Ranges at the Fleurieu Peninsula and extending onto Kangaroo
95 Island. The basin began as an intracontinental rift system that successfully progressed
96 to a passive margin basin in its southeast region, yet remained a failed rift in the north
97 (Lloyd et al. 2022a, preprint). Deposition within the basin ceased during the Delamerian
98 orogeny c. 514–490 Ma (Drexel & Preiss 1995; Foden et al. 2006; Foden et al. 2020;
99 Preiss 2000). Whilst present day exposure of the sedimentary basin is approximately
100 600 km north to south, the basin spans over 1,100 km from central Australia through to
101 Kangaroo Island. The stratigraphy of the Adelaide Superbasin is divided into three
102 supergroups (Lloyd et al. 2020; Preiss 2000), two for the Neoproterozoic sequences and
103 the third for the Cambrian sequences, with numerous group and subgroup level
104 divisions. The Warrina Supergroup is comprised of the Callanna, Burra, and Poolamacca
105 Groups, and the Heysen Supergroup contains the Umberatana, Wilpena, Torrowangee,
106 and Farnell Groups. Each of these groups are further divided into numerous subgroups.
107 Here we focus on the Yudnamutana Subgroup [Figure 2, Figure 3], which represents the
108 *Sturtian* glaciation, and present an additional sample from the overlying Nepouie
109 Subgroup, both are constituents of the Umberatana Group. One further sample is
110 presented from the thought to be equivalent Yancowinna Subgroup (NSW). The reader
111 is referred to Preiss (1987), Preiss (2000), Counts (2017), Lloyd et al. (2020), Cowley
112 (2020) and references therein for further detail on the geological history of the Adelaide
113 Superbasin.



114

115

116

Figure 2 – Stratigraphic table showing past (Preiss et al. 1998) and current correlations (this study) of the Yudnamutana Subgroup.

117

2.1.1 Yudnamutana Subgroup

118

119

120

121

122

123

124

125

126

127

128

129

130

131

132

133

134

135

136

The Yudnamutana Subgroup (Coats & Preiss 1987; Preiss et al. 1998; Thomson et al. 1964) is the lowermost subdivision of the Umberatana Group and is comprised of sedimentary rocks that represent the *Sturtian* glacial event in South Australia. The glaciogenic nature of these rocks was first recognised by Howchin (1901), and were traced during the early 20th century throughout the Mount Lofty, Flinders, and Olary Ranges (Preiss et al. 2011). A significant corpus of research has been published of over the past century (e.g., Coats & Forbes 1977; Conor & Preiss 2019; Cox et al. 2013; Cox et al. 2018b; David 1906; Fanning & Link 2008; Forbes & Cooper 1976; Howchin 1901; 1904; 1906; 1908; 1920; Le Heron et al. 2014; Le Heron et al. 2011; Link & Gostin 1981; Mawson & Sprigg 1950; Preiss 1987; 2000; Preiss et al. 1998; Preiss et al. 2011; Preiss et al. 1978; Segnit 1939; Sprigg 1952; Sweet & Preiss 1966; Thomson et al. 1964; Virgo et al. 2021) on the nature of these formations, with the “tillites” quickly rising to international fame (Cooper, BJ 2010; David 1906; Howchin 1908; and references therein). The most characteristic lithofacies of the Yudnamutana Subgroup are the diamictites, which have clasts ranging in size up to boulders. The matrix varies from mudstone, through to silty sands and abundant carbonates in some places. Siltstone with lone-stones and drop-stones are commonly associated with the diamictites, as are sandstones of varying compositions. Non-diamictite conglomerates are a minor lithofacies of the Yudnamutana Subgroup (Preiss et al. 2011). Sedimentary

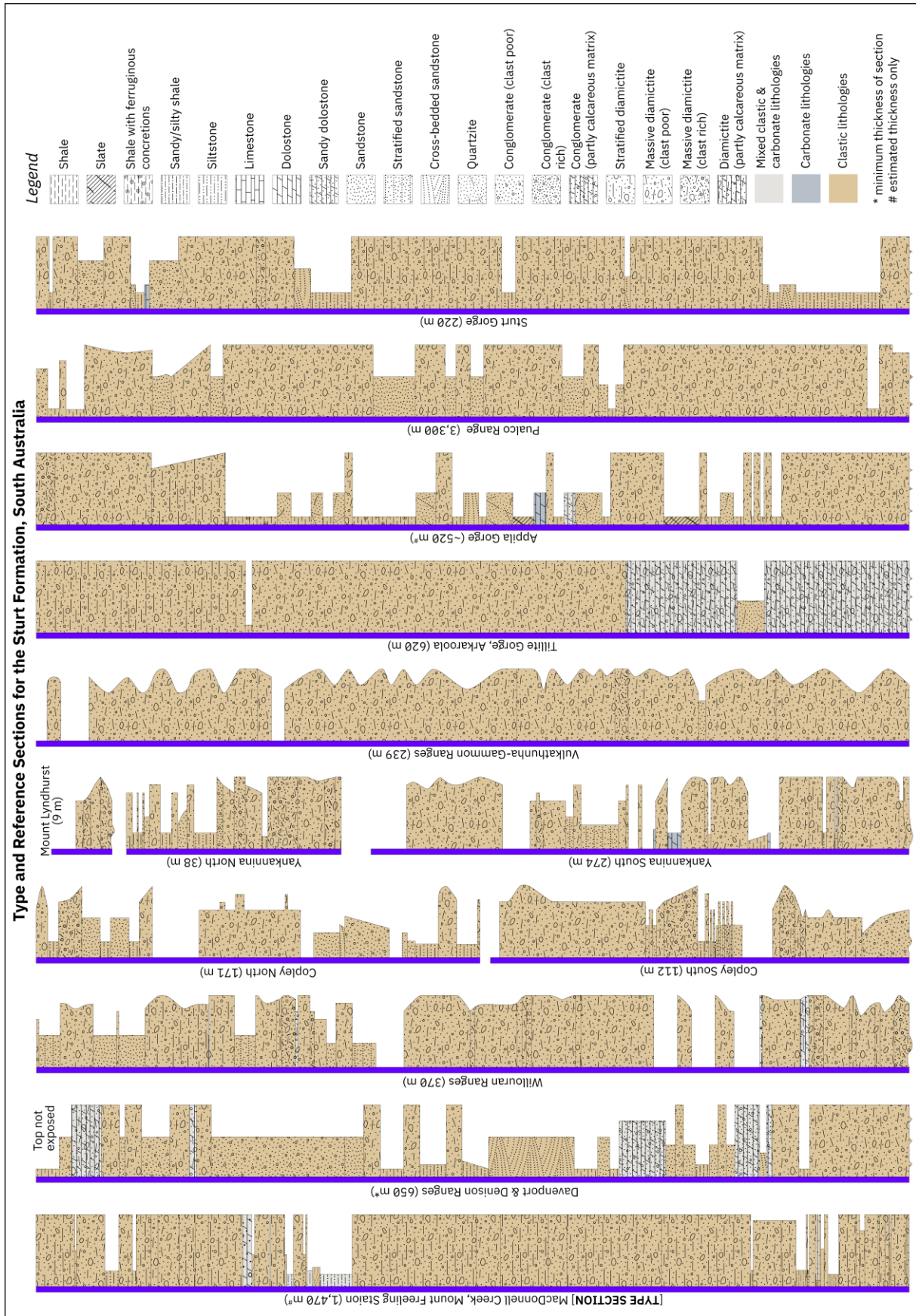


Figure 3 – Generalised stratigraphic logs of the Sturt Formation at its type section, and additional reference sections. For coordinates of locations see the accompanying stratigraphic unit definition (appendix). Copley, Yankannina, Willouran Ranges, and Vulkathuhna-Gammon Ranges sections are from logging done by authors in this study. Type section is based on data from Belperio (1973) and Young and Gostin (1989b). Other sections are compiled from Segnit (1939), Forbes and Cooper (1976), Coats and Preiss (1987), and Link (1977).

138 2011) in the eastern portion of the Adelaide Superbasin.

139 The Fitton Formation, only present in the northern Flinders Ranges, represents glacial
140 advance (Preiss et al. 1998; Young & Gostin 1989b). Currently there are six named
141 diamictite/tillite formations that represent the glacial maximum: the Appila Tillite
142 (Thomson et al. 1964) (based on the section of Segnit 1939), Bolla Bollana Tillite (Coats
143 & Forbes 1977; Thomson et al. 1964), Calthorinna Tillite (Ambrose et al. 1981),
144 Merinjina Tillite (Coats & Preiss 1987), Pualco Tillite (Forbes & Cooper 1976), and Sturt
145 Tillite (Howchin 1920; Mawson & Sprigg 1950). For the reasons outlined later in this
146 publication, the formations representative of the glacial maximum are here renamed the
147 Sturt Formation. The Benda Siltstone, Old Boolcoomata Conglomerate and Holowilena
148 Ironstone overlie the Sturt Formation but are limited in distribution (Conor & Preiss
149 2019; Lechte & Wallace 2015; Preiss 2006). The exact stratigraphic correlation of these
150 units is still uncertain but are likely partial equivalents of both underlying and overlying
151 stratigraphy. The Wilyerpa Formation (Dalgarno & Johnson 1966; Forbes 1971;
152 Thomson et al. 1964) and Lyndhurst Formation (Thomson et al. 1964; Young & Gostin
153 1989b) are the uppermost units of the Yudanamutana Subgroup and represent the
154 waning of the *Sturtian* glacial event (Preiss 1987; Preiss et al. 1998).

155 2.1.2 Yancowinna Subgroup

156 The Yancowinna Subgroup, Torrowangee Group, of western New South Wales, was
157 defined by (Cooper, PF & Tuckwell 1971) presented in further detail by (Cooper, PF et al.
158 1974). It consists of a sequence of coarse ill-sorted and clastic material namely arkose,
159 quartzite, sandstone, siltstone, conglomerate, and diamictite (Cooper, PF et al. 1974;
160 Fitzherbert & Downes 2015; Preiss 1987). True tillite has only been recognised in one
161 area (Cooper, PF 1973), but many of the facies closely resemble the possible
162 equivalents in South Australia (Preiss 1987). Its stratigraphic position supports an
163 equivalence with the Yudanamutana Subgroup of South Australia, with the Yancowinna
164 Subgroup overlain by the Euriowie Subgroup (inter-glacial) that is in turn overlain by the
165 Teamsters Creek Subgroup, which is thought to represent the Marinoan glacial event
166 (Fitzherbert & Downes 2015; Preiss 1987). Aside from detailed mapping and the
167 original sedimentological work, there is extraordinarily little research on these
168 sequences, and no geochronology has been published to date. As such the correlations
169 are likely, but uncertain.

170 2.1.3 Nepouie Subgroup

171 The inter-glacial Nepouie Subgroup most notably includes the basin-wide Tapley Hill
172 Formation. Other formations in the Nepouie Subgroup are the Brighton Limestone,
173 Balcanoona Formation, and Serle Conglomerate. The stratigraphic position is well
174 established for the Brighton Limestone and Balcanoona Formation, as both overlie the
175 Tapley Hill Formation. The Balcanoona Formation is coeval with the upper Tapley Hill
176 Formation, forming large palaeo-reef systems above it and passing laterally into it
177 (Wallace et al. 2015). The Tapley Hill Formation itself is primarily comprised of well

178 sorted, often calcareous, dolomitic, or pyritic shale. While extensive in both distribution
179 (basin-wide) and uniformity, there are several minor lithofacies that occur within the
180 Tapley Hill Formation, including arkose, greywacke, siltstone, dolostone, and lenticular
181 conglomerate beds. The latter is attributed to debris flows reworking the underlying
182 glaciogenic sequences (Preiss 1987). The only formation of the Nepouie Subgroup with
183 a still somewhat uncertain stratigraphic position is the Serle Conglomerate, however a
184 position conformably below the Tapley Hill Formation seems likely (Dyson 1996; 2004;
185 Preiss et al. 1998; Young & Gostin 1989a). The Serle Conglomerate is thought to be
186 deposited as part of a submarine fan complex (Young & Gostin 1989a).

187 2.2 Sturtian glaciation

188 The term *Sturtian* was originally used to describe a chronostratigraphic sequence in
189 South Australia and proposed for use as a global chronostratigraphic division by Dunn et
190 al. (1971). However, this has since been superseded by international nomenclature
191 (Gradstein et al. 2005; Knoll et al. 2006; Lloyd et al. 2020; Plumb 1991; Preiss et al.
192 2011; Shields-Zhou et al. 2016; Shields et al. 2022) with the *Sturtian* glaciation wholly
193 within the Cryogenian Period (Plumb 1991; Shields-Zhou et al. 2016). At present,
194 *Sturtian* is informally used by the international community as the name for the older of
195 two *snowball* (or *slushball*) Earth events (Fairchild & Kennedy 2007; Hoffman et al.
196 2017a; Hoffman et al. 1998; Hoffman & Schrag 2002) proposed to have occurred during
197 the Cryogenian. In a split from the growing consensus, Le Heron et al. (2020) have
198 advocated that the name “Laurentian Neoproterozoic Glacial Interval” be used in favour
199 of the *Sturtian*, and *Sturtian* be restricted to the formations in Australia, a concept we
200 are not in favour of and will discuss later.

201 The global distribution of pre-Cambrian glacial sequences, those now attributed to the
202 *Sturtian* glaciation, was recognised nearly a century ago (Hoffman 2011; Hoffman et al.
203 2017a, and references therein); however, synchronicity has only become evident within
204 the past two decades (e.g., Cox et al. 2018b; Dempster et al. 2002; Hoffman et al.
205 2017a; Keeman et al. 2020; Kendall et al. 2006; Lamothe et al. 2019; Lloyd et al. 2020;
206 Macdonald et al. 2010; Miller 2013; Park et al. 2019; Rooney et al. 2014; Rooney et al.
207 2015; Rooney et al. 2020; Shields et al. 2018; Xu et al. 2009). The recognition of global
208 time equivalence led Hoffman et al. (2017a) to propose calling the Cryogenian glacial
209 periods ‘cryochrons’. Advancements in the application of geochronology and mass
210 spectrometry have led to tight constraints on the global major onset of glaciation and
211 deglaciation c. 717 Ma and c. 660 Ma respectively (Hoffman et al. 2017a; Rooney et al.
212 2015).

213 3 Methods

214 Fifteen samples [Figure 1] from the Yudnamutana Subgroup (FR1_005_02,
215 FR1_009_01, FR2_007_01, FR2_024_01, FR3_005, FR3_006, FR3_009, FR3_034,
216 FR3_065, FR3_073, FR3_084a, FR3_109, FR3_139, ML_017, & ML_018), one sample
217 from the equivalent Yancowinna Subgroup (GSNSWKB002), and one sample from the

218 lowermost Nepouie Subgroup (FR3_004), were analysed for detrital zircon
219 geochronology.

220 Methodology is exactly that of (Lloyd et al. 2022a, preprint), with a summary provided
221 here.

222 Rock samples were prepared for detrital zircon analysis by crushing, sieving, panning
223 and, where necessary due to low zircon yield, heavy liquid separation. Any grain that
224 remotely resembled a zircon was picked to minimise human bias, an issue highlighted
225 by Sláma and Košler (2012) and Dröllner et al. (2021). Where permitted by zircon yields,
226 at least 300 zircons were picked per sample, otherwise all zircons in the sample were
227 picked. Cathodoluminescence images were obtained on either a FEI Quanta 600
228 scanning electron microscope (for zircon analysed in 2020) or a Cameca SXFive
229 Electron Microprobe (for zircon analysed in 2021). The zircons were using Laser
230 Ablation Inductively Coupled Plasma Mass Spectrometry (LA-ICP-MS) to obtain a suite
231 of elemental data for U–Pb geochronology and rare earth element (REE) analysis. All
232 zircons were analysed using a Resonetics M-50 (193 nm ArF excimer) laser ablation
233 system coupled with an Agilent 7900x inductively coupled plasma mass spectrometer.
234 All analytical instruments used are housed at Adelaide Microscopy, University of
235 Adelaide, Australia.

236 GJ-1 (Horstwood et al. 2016; Jackson et al. 2004), was used as the primary calibration
237 standard for U–Pb ratios and NIST610 (Jochum et al. 2011) was used as the primary
238 calibration standard for Pb isotope ratios and trace element data. The internal standard
239 for trace element data was set to ^{91}Zr with a value of 431,400 ppm (43.14 wt%)
240 assigned to unknowns. Plešovice (Horstwood et al. 2016; Sláma et al. 2008) and 91500
241 (Horstwood et al. 2016; Wiedenbeck et al. 1995; Wiedenbeck et al. 2004) were used as
242 validation standards. Unknowns were bracketed by two analyses of GJ-1, followed by a
243 combined two to three analyses of Plešovice and 91500, and two analyses of NIST610
244 every 20–30 unknowns. A 30 second gas blank followed by either a 40 second or 30
245 second ablation (session on 2021-03-30) time was used with a laser repetition rate of 5
246 Hz. A spot size of 29 μm and a nominal fluence of 2 Jcm^{-2} was used for zircon, and a
247 spot size of 43 μm using a nominal fluence of 3.5 Jcm^{-2} was used for NIST610. Data
248 were processed using LADR (Norris & Danyushevsky 2018), version 1.1.06 and output
249 as “Full Analytical Uncertainty”. No common Pb corrections were applied to the data.
250 Reference material ratios for GJ-1, Plešovice, and 91500 were set to the Chemical
251 Abrasion Isotope Dilution Thermal Ionisation Mass Spectrometry (CA-ID-TIMS) values
252 (uncorrected for thorium disequilibria and common-Pb) of Horstwood et al. (2016).
253 Weighted averages and dispersion statistics for all standards are available from the link
254 in data availability.

255 Statistical analysis of the zircon U–Pb data follows the method of Lloyd et al. (2020).
256 Data are considered concordant if within $\pm 10\%$, and a “meaningful” age if the 2σ
257 uncertainty is $\leq 10\%$ —if a datum satisfies both parameters it is termed a *Filtered Age*.
258 Maximum depositional ages are determined from a stricter 2% concordance filter and
259 use the older age of the three isotope ratios ($^{207}\text{Pb}/^{235}\text{U}$, $^{206}\text{Pb}/^{238}\text{U}$, $^{207}\text{Pb}/^{206}\text{Pb}$) for a

260 conservative estimate of the youngest single concordant grain. All ages are quoted with
261 2σ uncertainty. Kernel density estimates (KDEs), and multidimensional scaling plots
262 (MDS) were generated using IsoplotR (Vermeesch 2018). Key zircon trace element data
263 are presented graphically using methods following Verdel et al. (2021) and additionally
264 lanthanoid data are represented using violin plots and lambda representation
265 (Anenburg 2020; O'Neill 2016).

266 Metadata for the LA-ICP-MS sessions, data for all analyses, cathodoluminescence
267 images, and R code used to generate plots are available from the links in data and code
268 availability.

269 4 Results

270 Fifteen samples [Figure 1] from the Yudnamutana Subgroup (FR1_005_02,
271 FR1_009_01, FR2_007_01, FR2_024_01, FR3_005, FR3_006, FR3_009, FR3_034,
272 FR3_065, FR3_073, FR3_084a, FR3_109, FR3_139, ML_017, & ML_018), one sample
273 from the equivalent Yancowinna Subgroup (GSNSWKB002), and one sample from the
274 lowermost Nepouie Subgroup (FR3_004), were analysed for detrital zircon
275 geochronology. Several samples had naturally low zircon yields (FR3_004,
276 FR1_005_02, GSNSWKB002, FR3_084a, FR3_139, Fitton Formation samples).

277 4.1 Fitton Formation

278 A cumulative total of 124 analyses, with 95 analyses passing filtering parameters, were
279 conducted for samples FR3_065 (92/74), FR3_009 (9/1), and FR2_024_01 (23/20).
280 The data for these samples are combined as only two samples yield more than one
281 filtered analysis. These two samples are ~200 m apart (geographically), all three
282 samples are from the broader local area [Figure 1], and there are no discernible
283 differences in the age spectra. Ages range from 1134 ± 24 Ma to 2458 ± 37 Ma, with as
284 primarily population peak c. 1580 Ma, and a secondary peak c. 1160 Ma [Figure 4].

285 4.2 Sturt Formation and equivalents

286 A cumulative total of 162 analyses, with 107 analyses passing filtering parameters,
287 were conducted on zircon from samples ML_017 (117/93) and ML_018 (45/14), South
288 Mount Lofty Ranges (Sturt Gorge, Adelaide). The data for these samples are combined
289 as the two sampling sites are ~60 m apart (geographically) [Figure 1] and there are no
290 discernible differences in the age spectra. Ages range from 930 ± 16 Ma to 2933 ± 34
291 Ma, with a primary population peak c. 1840 Ma, tailing towards 1560 Ma. An additional
292 minor population peak is present c. 1100 Ma [Figure 4].

293 A total of 178 zircons were analysed from sample FR1_009_01, North Mount Lofty
294 Ranges, with 98 passing filtering parameters. Ages range from 1501 ± 48 Ma to $3374 \pm$
295 32 Ma, with a single population peak c. 1790 Ma [Figure 4].

296 A cumulative total of 81 analyses, with 77 analyses passing filtering parameters, were

297 conducted on zircon from samples
 298 FR2_007_01 (31/28) and FR3_139
 299 (50/49), North Flinders Ranges
 300 (Copley area) [Figure 1]. The data for
 301 these samples are combined as they
 302 were sampled from the same
 303 stratigraphic interval at
 304 approximately the same
 305 stratigraphic height. Ages range
 306 from 663 ± 11 Ma to 2718 ± 21 Ma,
 307 with a primary population peak c.
 308 1740 Ma and secondary population
 309 peaks c. 1580 Ma, 1180 Ma, and
 310 1050 Ma [Figure 4].

311 A cumulative total of 52 analyses,
 312 with 46 analysed passing filtering
 313 parameters were conducted on
 314 zircon from FR3_084a (10/9) and
 315 FR3_109 (42/37), North Flinders
 316 Ranges (Yankaninna area). The data
 317 from these two samples is combined
 318 as they are sampled from within 30
 319 metres of each other in the same
 320 interval of outcrop [Figure 1]. Ages
 321 range from 1042 ± 19 Ma to $2514 \pm$
 322 48 Ma, with a single primary
 323 population peak c. 1640 Ma [Figure
 324 4].

325 A total of 118 zircons were analysed
 326 from sample FR3_073, North
 327 Flinders Ranges (Vulkathuhna-
 328 Gammon Ranges) [Figure 1], with 94
 329 passing filtering parameters. Ages
 330 range from 891 ± 15 Ma to $3322 \pm$
 331 35 Ma, with a single broad, and
 332 slightly bimodal population peak
 333 range of c. 1740 Ma to c. 1620 Ma
 334 [Figure 4].

335 A total of 144 zircons were analysed
 336 from sample FR3_034, North Flinders
 337 Ranges (Stubbs Waterhole, Arkaroola),
 338 with 125 passing filtering parameters.
 Ages range from 1117 ± 34 Ma to
 2691 ± 42 Ma, with a primary
 population peak c. 1590 Ma, and a
 secondary population peak c. 1750 Ma
 [Figure 4].

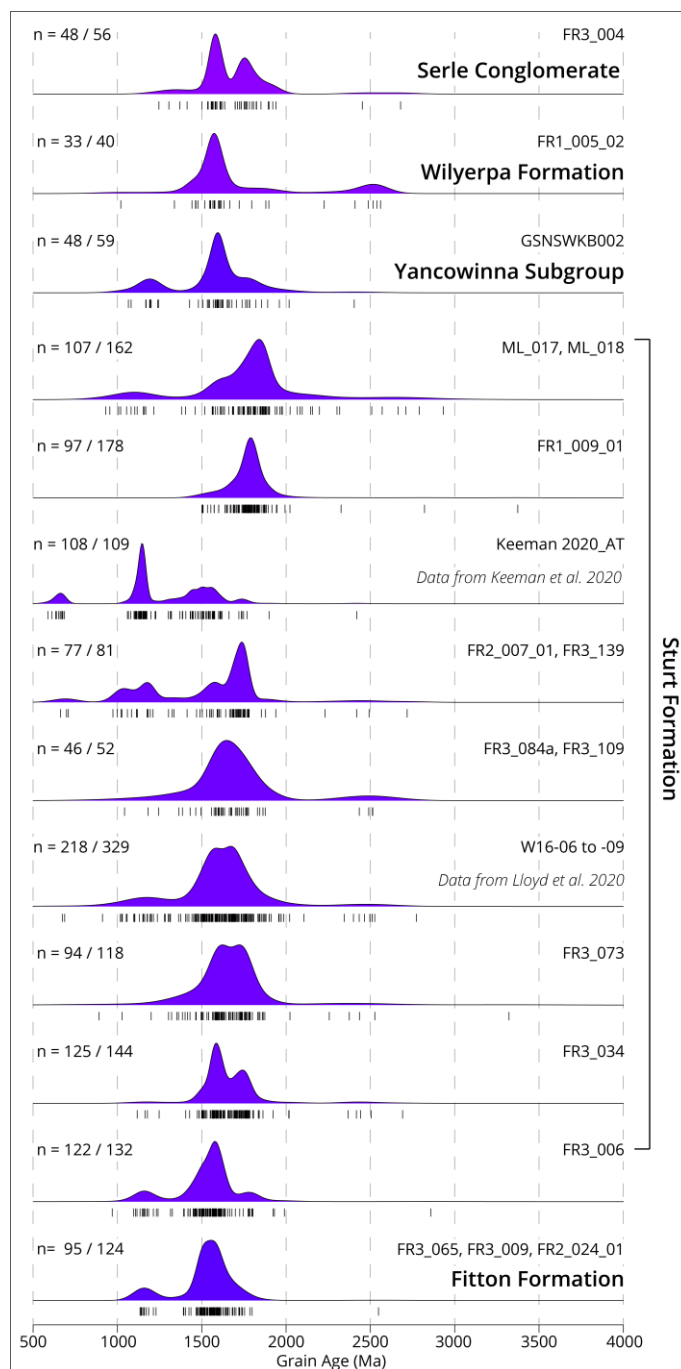


Figure 4 – Kernel density estimates [KDEs] of detrital zircon populations from Yundnamutana, Yancowinna and Nepouie Subgroup samples. Data are from this study unless otherwise denoted. Tick marks below each plot represent an analysis. n = filtered analyses / total analyses. Generated using IsoplotR (Vermeesch 2018).

339 A total of 132 zircons were analysed from sample FR3_006, North Flinders Ranges
340 (Stanley Mine, Arkaroola) [Figure 1], with 122 passing filtering parameters. Ages range
341 from 969 ± 16 Ma to 2858 ± 47 Ma, with a primary population peak c. 1580 Ma, and
342 secondary population peaks c. 1790 Ma and 1160 Ma [Figure 4].

343 A total of 59 zircons were analysed from sample GSNSWKB002, Yancowinna Subgroup,
344 Koonenberry Belt (New South Wales) [Figure 1], with 48 passing filtering parameters.
345 Ages range from 1065 ± 18 Ma to 2404 ± 37 Ma [Figure 4].

346 4.3 Lyndhurst and Wilyerpa Formations

347 Sample FR3_005, Lyndhurst Formation, had extremely low zircon yield with only three
348 zircons obtained and analysed. Of those, only two passed filtering parameters, with
349 ages of 1532 ± 24 Ma and 1174 ± 19 Ma [Figure 4].

350 A total of 40 zircons were analysed from sample FR1_005_02, Wilyerpa Formation,
351 North Mount Lofty Ranges [Figure 1]. Of these, 33 passed filtering parameters with ages
352 ranging from 1020 ± 19 Ma to 2560 ± 79 Ma, with a primary population peak c. 1580
353 Ma and a secondary population c. 2500 Ma [Figure 4].

354 4.4 Serle Conglomerate

355 A total of 56 zircons were analysed from sample FR3_004, Serle Conglomerate, with 48
356 passing filtering parameters. Ages range from 1246 ± 24 Ma to 2679 ± 65 Ma, with a
357 primary population peak c. 1590 Ma, and a secondary population peak c. 1760 Ma
358 [Figure 4].

359 4.5 Zircon trace element 360 geochemistry

361 Most analyses resolved lanthanoid
362 concentrations that are typical for
363 zircons, with several orders-of-
364 magnitude increase in concentration
365 from light to heavy elements, a
366 slight negative deviation in
367 europium (Eu), and a positive
368 deviation in cerium (Ce) [Figure 5].
369 However, two analyses
370 (FR1_009_01b – 057, and
371 FR1_009_01 - 044) have lanthanoid
372 concentrations atypical of zircon,
373 with overall positive (based on ionic
374 radii) slopes (λ_1 of +7.14, and +1.06)
375 due to highly elevated light
376 lanthanoids (La to Nd). Overall, the

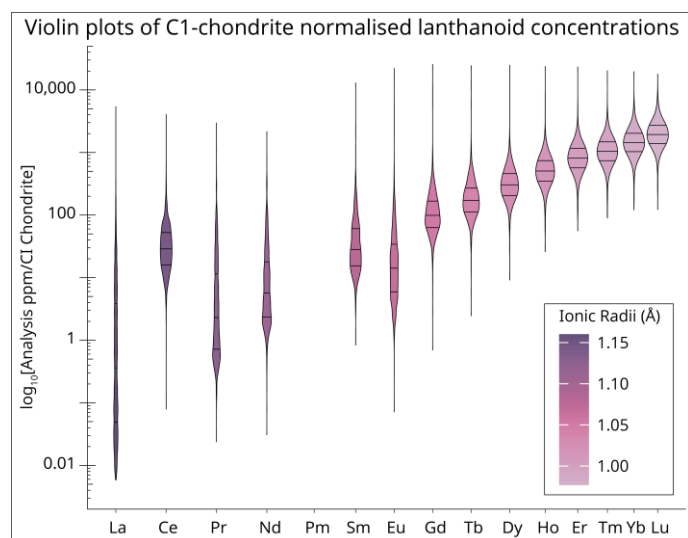


Figure 5 – Violin plots of CI chondrite (O'Neill 2016) normalised lanthanoids for all filtered zircon analysed in this study. X-axis is spaced by ionic radii (Shannon 1976) and ordered by atomic number. Black lines across the fill of each plot represent the 0.25, 0.5, and 0.75 quantiles. Bandwidth of the density estimates is calculated using the Botev algorithm from the Provenance package (Vermeesch et al. 2016).

377 lanthanoid pattern for both analyses have a concave-up shape with heavy lanthanoid
378 concentration increasing as would normally occur in zircon. Major element percentages,
379 ~14.4 wt% and ~15.6 wt% silicon, suggest these two analyses are zircon, and CL
380 images also support this, although show patchy textures. The ages for these are at the
381 limit of discordance acceptance (90%). It is likely these two analyses have gone through
382 complicated zones of inclusions, altered metamict zones, and/or mineral overgrowths.

383 5 Discussion

384 5.1 Zircon trace element geochemistry

385 A simple U/Yb against Y plot can be
386 used to infer continental or oceanic
387 affinity for zircon generation
388 (Grimes et al. 2007; Grimes et al.
389 2015). Most zircons analysed in this
390 study are inferred to have been
391 generated in continental crust
392 [Figure 6], with a small number of
393 younger zircons suggesting oceanic
394 affinity. C1 chondrite normalised
395 (O'Neill 2016) concentrations of
396 lanthanoids are generally typical of
397 zircon [Figure 5] with a positive
398 pattern slope (increasingly negative
399 λ_1 values) from light to heavy
400 lanthanoids, a positive cerium
401 anomaly, and negative europium
402 anomaly (Hoskin & Ireland 2000;
403 Hoskin & Schaltegger 2003). Nearly
404 all zircons have a Th/U >0.07 and
405 are generally inferred to be
406 originally generated as magmatic
407 rather than metamorphic zircon (Rubatto 2002). There is no apparent trend in
408 lanthanoid pattern slope or curvature [Figure 7], denoted as λ_1 (linear slope), λ_2
409 (quadratic slope), and λ_3 (cubic slope) (Anenburg 2020), with time or sample. Both Eu
410 and Ce anomalies (denoted by Eu* and Ce*) show a significant spread through time. The
411 youngest few zircons c. 670 Ma, although limited in number, have out of phase Eu* (low)
412 and Ce* (high) anomalies suggestive of growth in competition with plagioclase, and not
413 reflective of magma oxidation state (Verdel et al. 2021).

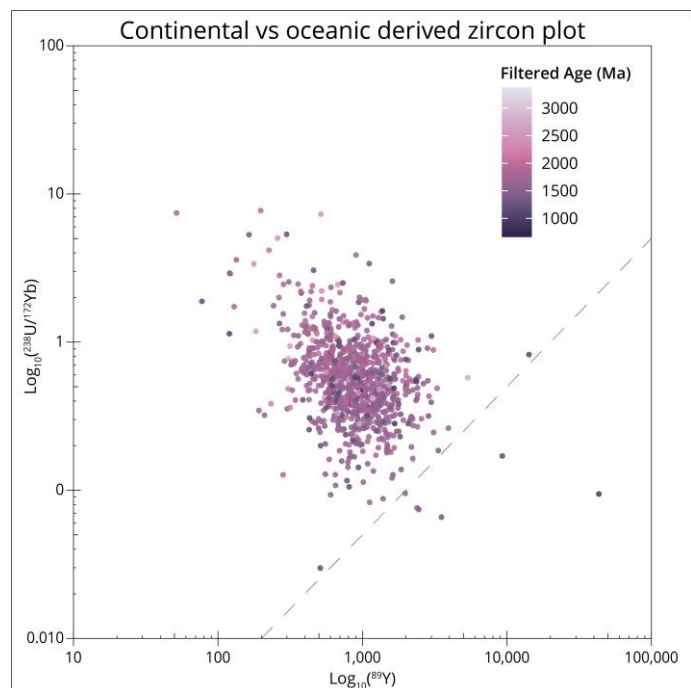


Figure 6 – Plot based on (Grimes et al. 2007) used as an indicator of zircon crustal origin. This plots Y against U/Yb, with the dashed reference line dividing the “oceanic” (below line) and “continental” (above line) fields. Most data plot above the reference line, suggesting zircon formation mostly in crust of continental affinity. Coloured by filtered age where light is older and darker is younger.

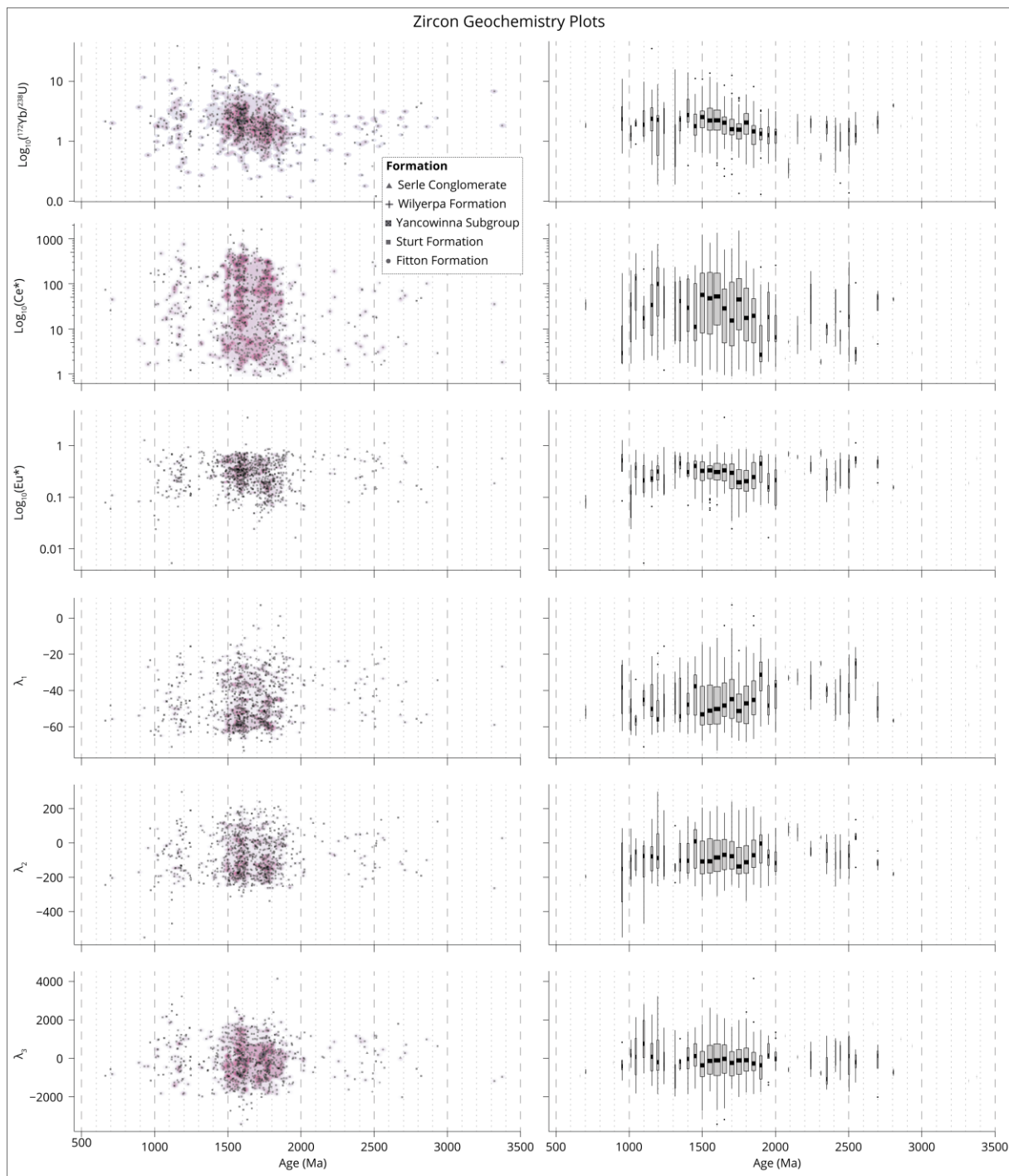


Figure 7 – Key zircon geochemistry plots for zircon analysed in this study. Left: Scatter plots underlain with 2D density estimation. Right: 50 million year binned boxplots with width scaled by the count of values in the bin. Top to bottom: Yb/U, Ce*, Eu* and λ_1 –3. λ_1 –3 are measures of lanthanoid pattern shapes, with λ_1 –3 representing the linear slope, quadratic slope and cubic slope respectively. Ce*, Eu* and λ_1 –3 are calculated using BLambdaR (Anenburg & Williams 2021).

415 5.2 Provenance and maximum depositional ages

416 5.2.1 Maximum depositional ages

417 The older limit of expected depositional age for samples in this study is constrained by
418 two MDA constraints from the underlying Belair Subgroup, namely the Gilbert Range
419 Quartzite (731 ± 34 Ma, Keeman et al. 2020; Lloyd et al. 2020) and Mitcham Quartzite
420 (c. 730 Ma, Lloyd et al. 2022c, preprint; van der Wolff 2020). The younger age limit for
421 deposition of the Yudnamutana Subgroup is constrained by a 663 ± 0.76 Ma tuff in the
422 Wilyerpa Formation (Cox et al., 2018). The Serle Conglomerate is older than c. 642 Ma
423 Tapley Hill Shale (Re-Os shale, Kendall et al. 2006) which is interpreted to underlie.

424 A maximum depositional age (MDA) of 1162 ± 49 Ma was obtained for the combined
425 Fitton Formation samples. This is significantly older than the expected depositional age
426 c. 663–730 Ma.

427 Maximum depositional ages for each of the Sturt Formation samples are presented here
428 according to the combinations outlined in 4.2.

- 429 • South Mount Lofty Ranges (Sturt Gorge, Adelaide): 1007 ± 14 Ma
- 430 • North Mount Lofty Ranges (Clare Valley): 1774 ± 39 Ma
- 431 • North Flinders Ranges (Copley area): 666 ± 25 Ma
- 432 • North Flinders Ranges (Yankaninna area): 1186 ± 50 Ma
- 433 • North Flinders Ranges (Vulkathuhna-Gammon Ranges): 891 ± 15 Ma
- 434 • North Flinders Ranges (Stubbs Waterhole, Arkaroola): 1188 ± 51 Ma
- 435 • North Flinders Ranges (Stanley Mine, Arkaroola): 1118 ± 48 Ma

436 Previous MDAs obtained from detrital zircon studies (Keeman et al. 2020; Lloyd et al.
437 2020) on the Sturt Formation are:

- 438 • South Mount Lofty Ranges (Sturt Gorge, Adelaide): 714 ± 28 Ma
- 439 • South Flinders Ranges (Pichi Richi Pass): 667 ± 6 Ma
- 440 • North Flinders Ranges (Willouran Ranges): 673 ± 19 Ma

441 There is significant scatter in the MDAs of individual samples; however, population
442 spectra are similar [Figure 4, Figure 8] across all samples (spanning more than 500 km
443 north–south, Figure 1), and three independent sets of samples over a distance of ~250
444 km north–south, have MDAs within uncertainty of each other. While detrital zircon
445 population spectra variations occur locally, as is expected across a large basin, and with
446 significant recycling of underlying stratigraphy in glaciogenically derived sediment, the
447 remarkable similarity of most samples' spectra [Figure 4, Figure 8] adds support to unit
448 equivalence, as is strongly suggested by lithostratigraphy. The variation in MDAs also
449 highlights the main challenge in determining depositional ages via detrital zircon studies
450 as it is entirely possible for the MDA to be significantly older than the true age of
451 deposition. This is both a factor of chance (sampling) and dependant on original
452 sediment input—if no zircon of syndepositional ages are present in the detritus being fed
453 into the depocentre, the true age of deposition cannot be determined by this method,

465 1987). The sample is as a highly weathered diamictite with clasts ranging up to pebble
466 size, and a silty to fine sand matrix. This was a reconnaissance sample with the aim to
467 investigate the general correlation of this subgroup to the Yudnamutana Subgroup of
468 South Australia. An MDA of 1075 ± 40 Ma was obtained from the sample, with a detrital
469 zircon population spectrum similar to that of the likely correlatives in South Australia
470 [Figure 4, Figure 8]. This provides limited, but supporting evidence of a shared detrital
471 source and that these two subgroups are correlative as is indicated by the existing
472 lithostratigraphic framework (Lloyd et al. 2020).

473 An MDA of 1502 ± 70 Ma was obtained from the Wilyerpa Formation (FR1_005_02)
474 sampled in the Clare Valley. This is significantly older than the expected depositional
475 age c. 663 Ma and may be a factor of low zircon yield and/or no zircon close to
476 depositional age being present in the sample.

477 An MDA of 1291 ± 50 Ma was obtained from the Serle Conglomerate sample (FR3_004).
478 Again, this is significantly older than true depositional age that is expected to be
479 between c. 663 Ma and c. 642 Ma. The detrital zircon population spectrum somewhat
480 differs [Figure 4, Figure 8] from the nearby Sturt Formation sample (FR3_006), although
481 this may partially be an artifact of the much lower zircon yield from the Serle
482 Conglomerate sample.

483 5.2.2 Provenance

484 Two broad detrital zircon populations, c. 1840–1790 Ma and c. 1640–1580 Ma, from
485 major peaks in virtually all samples. The exact age positions and magnitude of the
486 population peaks varies slightly by sample, with broad to north–south and east–west
487 variations, generally trending to older Palaeoproterozoic age populations in the west
488 and south. It is likely that there is significant recycling of the underlying stratigraphy due
489 to sub-glacial erosion (Young & Gostin 1989b). The similarity of the detrital zircon
490 spectra within the samples of this study to each other, and to earlier rocks of the
491 Adelaide Superbasin [Figure 8], suggests homogenisation of detrital material over a
492 large area, potentially with extra-basin material, and also supports the notion of intra-
493 basin recycling occurring from sub-glacial erosion of earlier stratigraphy.

494 Zircons with ages greater than ~1400 Ma are likely locally, from the Gawler
495 Craton/Barossa Complex and Curnamona Province that record numerous zircon
496 generation events and sedimentary sequences known to hold zircon of these ages
497 (Barovich & Hand 2008; Belousova et al. 2009; Conor & Preiss 2008; Fanning et al.
498 2007; Fraser et al. 2010; Fraser & Neumann 2010; Jagodzinski & Fricke 2010;
499 Jagodzinski & McAvaney 2017; Jagodzinski et al. 2020; Kromkhun et al. 2013;
500 McAvaney 2012; Meaney 2012; 2017; Morrissey et al. 2019; Morrissey et al. 2018;
501 Morrissey et al. 2013; Reid, A et al. 2021; Reid, Anthony J et al. 2019; Reid, Anthony J.
502 & Hand 2012; Reid, Anthony J. et al. 2008; Reid, Anthony J. et al. 2014a; Reid, Anthony
503 J. et al. 2014b; Reid, Anthony J. et al. 2017; Reid, Anthony J. & Payne 2017; Stevens et
504 al. 2008; Swain et al. 2005; Wade, CE 2011). The southernmost samples from Sturt
505 Gorge are dominated by c. 1840 Ma zircons, and northward progression generally sees a

506 shift in dominance of the c. 1840 Ma population to the younger c. 1580 Ma. This
507 observation is likely a result of the variation in local basement geology of the Gawler
508 Craton and Curnamona Province near the sample sites.

509 The generally minor Stenian population of zircon at c. 1160 Ma is suggestive of
510 provenance from the Musgrave Province (Smithies et al. 2008; Smithies et al. 2011;
511 Smits et al. 2014; Wade, BP et al. 2008), but as noted in (Lloyd et al. 2022a, preprint)
512 they may be sourced from an as yet undiscovered but inferred late Mesoproterozoic (c.
513 1300–1000 Ma) source to the east (Fergusson et al. 2007; Korsch et al. 2012; Mackay
514 2011; Wysoczanski & Allibone 2004). This population is generally more abundant in
515 samples closer to the eastern and western margins of the basin [Figure 4, Figure 1].
516 Alternate sources of these late Mesoproterozoic zircon could be the South Tasman Rise
517 (Fioretti et al. 2005), Coompana Province (Pawley et al. 2020) or far-field transport
518 across Antarctica from the Tonian Oceanic Arc Super Terrane (Jacobs et al. 2015).
519 Again, it is highly likely recycling of underlying stratigraphy is also a partial origin of
520 these zircons.

521 Neoproterozoic zircon of ages between c. 900 Ma and c. 780 Ma are feasibly attributed
522 to early known magmatism in the Adelaide Superbasin (Lloyd et al. 2020); however
523 those younger than 780 Ma are much more difficult to reconcile. It is apparent that
524 some zircon-bearing magmatic crystallisation of zircon was occurring c. 700 Ma to c.
525 660 Ma, and that these were in the sediment supply of the Sturt Formation. While a 663 ± 0.76 Ma tuff has been dated (Cox et al. 2018b) from within the Wilyerpa Formation,
526 immediately post-dating deposition of the Sturt Formation. The original volcanic centre
527 for the ashfall is unknown. Additionally, zircon of this age (c. 700–660 Ma), within the
528 Sturt Formation has so far, only been found on the far western margin of the Adelaide
529 Rift Complex within the Adelaide Superbasin [Figure 9], potentially suggesting this
530 magmatic source was to the west of, or on the western margin of the basin.
531

532 Comparison is made to three correlatives (Edgoose 2013; Kruse et al. 2013;
533 Normington & Donnellan 2020) from the Centralian Superbasin, the syn-glacial Yardida
534 Tillite and Areyonga Formation, and the post-glacial Aralka Formation. Interestingly, the
535 detrital zircon age spectra of the Yardida Tillite (Georgina Basin, Northern
536 Territory/Queensland) which is likely to be a correlative of the Sturt Formation, is very
537 similar [Figure 8] to the local basement of South Australia (e.g., Gawler Craton).
538 However, this is explained by its proximity to the Mount Isa and Aileron Provinces,
539 suggested to be the primary zircon source for the Yardida Tillite (Verdel et al. 2021).
540 These provinces host abundant c. 1640–1850 Ma zircon that are also found the Gawler
541 Craton and Curnamona Province. The age spectra in the Areyonga Formation and Aralka
542 Formations (Amadeus Basin, Northern Territory/Western Australia) are similar to Burra
543 Group formations and the Sturt Formation samples from the western margin of the
544 Adelaide Rift Complex. All of these aforementioned formations are suggested to
545 ultimately source zircon from the Musgrave province where Stenian-aged zircon are
546 abundant, and both basins have abundant nearby sources of pre-Stenian aged zircon.
547 Notably though no zircon younger than c. 800 Ma has been found in the Areyonga and
548 Aralka formations to date.

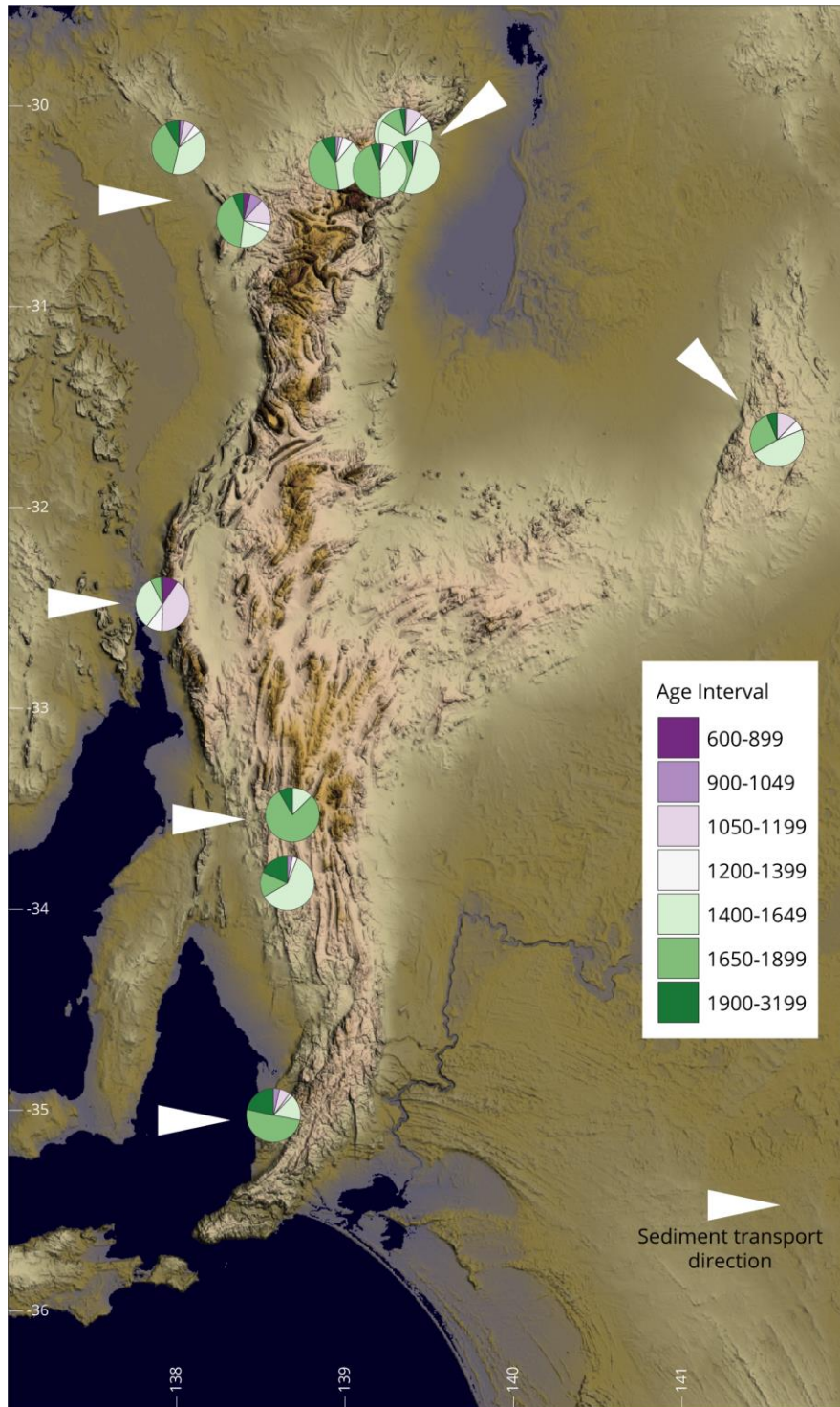


Figure 9 – Schematic map with pie charts at samples locations to highlight the changes in zircon population spectra relative to geographic location. Arrows are generalised and schematic indicators of palaeo-sediment transport direction.

549

550 5.2.3 Comparison to Palaeocurrent data

551 Observations drawn in this study from detrital zircon are generally supportive of existing
 552 palaeocurrent data (Link & Gostin 1981; Young & Gostin 1989b; 1991). Palaeocurrent

553 data from the Yudnamutana Subgroup suggest a westerly transport direction in the
554 Mount Painter area and along the Paralana fault system, northerly transport on the
555 northern side of the Gammon syncline and Yankaninna anticline, and north-easterly
556 transport along the eastern edge of the Adelaide Rift Complex (Copley area, south-
557 eastern Willouran Ranges). It is likely that underlying strata have been recycled, making
558 the use of detrital zircon spectra for determining palaeo-transport paths difficult;
559 however, the only area in which the detrital data from this study might potentially differ
560 in transport direction from the existing palaeocurrent data is the Vulkathuhna-Gammon
561 Ranges. Our data (Figure 4: FR3_073, Fitton Formation samples) may suggest a south,
562 or south-westerly sediment transport [Figure 9] direction as the detrital zircon
563 populations are similar to the older stratigraphy of the basin, and to the local basement
564 sources located to the northeast [Figure 8, Figure 1].

565 5.3 Tectonic and palaeogeographic implications

566 While the dataset needs to be expanded in future to cover more the basin, particularly
567 to the east (Olary area, and New South Wales) and far northwest (Davenport and
568 Denison Ranges), some points can be made regarding the palaeogeography and
569 tectonics of the Adelaide Superbasin during the *Sturtian glaciation*. Firstly, it is apparent
570 that the detrital zircon spectrum of each sample is highly dependent on local geology,
571 often recycling the underlying stratigraphy and/or from the nearby basement geology.
572 This finding suggests that the far-field sediment supply to the Burra Group (as inferred
573 by Lloyd et al. 2020) was shut off during deposition of the Yudnamutana Subgroup, with
574 locally derived detritus becoming much more prominent (Lloyd et al. 2020). Secondly,
575 active zircon-bearing magmatism occurred at c. 700–660 Ma, although the location and
576 volume of this magmatism remains unknown. The spatial distribution of the samples
577 containing Cryogenian zircon [Figure 9] suggests that the source was to the west, or
578 along the western margin, of the basin. Thirdly, the detrital zircon spectrum of the
579 Yancowinna Subgroup sample supports a shared sediment supply for it and the Sturt
580 Formation samples in the northeast of the basin, allowing for a topographic high
581 (Curnamona Province) in between these two areas that is shedding detrital material to
582 both sides. The data presented here also adds support to the Yancowinna Subgroup
583 being an equivalent of the Yudnamutana Subgroup, as is suggested by the current
584 stratigraphic framework (Cooper, PF 1973; Cooper, PF & Tuckwell 1971; Fitzherbert &
585 Downes 2015; Lloyd et al. 2020; Preiss 1987). In combination with glacial scouring, it is
586 likely that active tectonics played a significant control on the dramatic thickness
587 variations of the Yudnamutana Subgroup sedimentary rocks (Le Heron 2012; Le Heron
588 et al. 2014; Young & Gostin 1991), although this likely post-dates the rift-drift transition
589 of the Australia–Laurentia margin c. 780 Ma (Merdith et al. 2017).

590 5.4 Sturtian nomenclature

591 5.4.1 South Australian Formal Stratigraphy

592 The original correlations of the ‘older’ glacial units across southern Australia (e.g. Sturt

593 Tillite, Appila Tillite) were originally argued to represent either one or two separate
594 glacial intervals (Coats & Forbes 1977; Coats & Preiss 1987). Subsequent work showed
595 that they were all consistent with only one glacial event (Murrell et al. 1977; Preiss
596 1993; 2000; Preiss et al. 1998) but representing ice sheet advance-retreat cycles (Le
597 Heron 2012). No significant lithological differentiation (in the sense of formal
598 stratigraphy) can be made to distinguish them from one another (Preiss et al. 1998;
599 Preiss et al. 2011), and both stratigraphic position and geochronology supports their
600 equivalence (this study, Cox et al. 2018b; Keeman et al. 2020; Lloyd et al. 2020; Preiss
601 et al. 1998; Young & Gostin 1989b). In light of this knowledge, we redefine and combine
602 the stratigraphic nomenclature for the outcrops that represent the glacial maximum
603 (e.g., Appila Tillite, Bolla Bollana Tillite, Sturt Tillite) to the Sturt Formation [Figure 2].
604 *Sturt* is retained as the first diamictite formally named was the *Sturtian tillite* (Howchin
605 1920; Mawson & Sprigg 1950), as such it takes precedence over all other equivalent
606 formation names, and it has become internationally synonymous with the *Sturtian*
607 glaciation. *Tillite* has been dropped in favour of *Formation* as, while they are the most
608 distinctive lithology, the lithologies are not exclusively diamictites of glacial origin, and
609 they are not the most volumetrically abundant lithologies in all areas (Preiss et al.
610 2011). Instead, the Sturt Formation is comprised of numerous lithologies that were
611 deposited under general glacial conditions (Link 1977; Link & Gostin 1981; Preiss 1987;
612 2000; Preiss et al. 2011). A formal definition card accompanies this paper as an
613 appendix, with the generalised stratigraphic logs of the type and reference sections
614 presented in Figure 3.

615 5.4.2 Sturtian glaciation (Cryochron)/Laurentian Neoproterozoic Glacial 616 Interval

617 Le Heron et al. (2020) proposed that the name “Laurentian Neoproterozoic Glacial
618 Interval” be used in favour of the *Sturtian*, with the latter name used exclusively for
619 Australian strata. While they highlight the issue of interpreting results in a model-led
620 approach, a point we agree on, Le Heron et al. (2020) primarily base this on their
621 interpretation that most *Sturtian* rocks of Australia chronometrically lie outside of the
622 *Sturtian* glacial interval, c. 720–660 Ma, defined by Rooney et al. (2015), with only the
623 tuff from near the base of the Wilyerpa Formation (663.03 ± 0.76 Ma, Cox et al. 2018b)
624 plotting within this time interval, this is reiterated by Kennedy et al. (2020). However,
625 we argue that this interpretation is incorrect, as Le Heron et al. (2020) interpretation
626 appears to hinge on the previous lack of data from the South Australian Sturtian glacial
627 (Yudnamutana Subgroup) and pre-glacial (Burra Group) sequences. Since publication,
628 even with the challenges associated with constraining deposition by detrital zircon
629 studies, two studies (Keeman et al. 2020; Lloyd et al. 2020) have provided maximum
630 depositional age constraints from the Sturt Formation: South Mount Lofty Ranges, $714 \pm$
631 28 Ma; South Flinders Ranges, 667 ± 6 Ma; North Flinders Ranges, 673 ± 19 Ma. This
632 study presents a further ten samples, with FR3_139 yielding an MDA of 666 ± 25 Ma.
633 Importantly, detrital zircon MDA constraints from the underlying Belair Subgroup,
634 namely the Gilbert Range Quartzite (731 ± 34 Ma, Keeman et al. 2020; Lloyd et al.

635 2020) and Mitcham Quartzite (c. 730 Ma, Lloyd et al. 2022c, preprint; van der Wolff
636 2020) provide the maximum age estimations for which final deposition occurred within
637 the upper Burra Group. Le Heron et al. (2020) treat the Cox et al. (2018b) tuff age
638 (Wilyerpa Formation, AUS) as a maximum depositional age, although Cox et al. (2018b)
639 demonstrate that the tuff age is syndepositional, with their age dating volcanism coeval
640 with deglaciation. It neither provides a maximum or minimum age limit for the entire
641 Wilyerpa Formation as it occurs part way up section with ~50 additional stratigraphic
642 metres overlying the tuff to the base of the Tapley Hill Formation. This age provides a
643 robust minimum age construction for the underlying diamictite. Thus, these two
644 bracketing constraints require that the *Sturtian* glaciogenic rocks of South Australia
645 (Sturt Formation, Fitton Formation) are deposited c. ≤ 730 Ma and $\geq 663 \pm 0.76$ Ma,
646 thereby constraining the age of the true *Sturtian* (*sensu stricto*) to this time bracket. The
647 initiation of final deglaciation can also be constrained by the data presented here, albeit
648 loosely to between 666 ± 25 Ma and 663.03 ± 0.76 Ma, as samples FR3_139 and
649 FR2_007_01 come from the same stratigraphic interval as the tuff from the Wilyerpa
650 Formation. This independently aligns with the current definition for global timing of the
651 *Sturtian* glaciation, c. 717–660 Ma (Rooney et al. 2015).

652 By contrast Le Heron et al. (2020) treat the reworked tuff age from the Pocatello
653 Formation, USA (Fanning & Link 2004), as a minimum age estimate. This reworked tuff
654 of Fanning and Link (2004) from the “upper diamictite” (Isakson 2017) of the Pocatello
655 Formation has been reevaluated as a maximum depositional age and may actually be a
656 *Marinoan* glacial sequence, unconformably overlying a non-glacial sequence that in turn
657 unconformably overlies a lower *Sturtian* sequence (Isakson 2017). Isakson (2017) had
658 also revised several of the igneous ages presented in the Le Heron et al. (2020)
659 compilation, notably a syn-*Sturtian* age from the Hogback Rhyolite from 684 ± 4 Ma
660 (Lund et al. 2010; Lund et al. 2003) to 693.03 ± 0.73 Ma. This author also presented
661 two additional ages from volcanics in the lower Scout Mountain Member of the Pocatello
662 Formation of c. 697 Ma, previously interpreted to be 686 ± 4 Ma (Fanning & Link 2008).
663 The data of Keeley et al. (2013) from the lower Scout Mountain member (685 ± 0.4 Ma)
664 is presented as a depositional age by Le Heron et al. (2020), rather than as a maximum
665 depositional age as the original authors and Isakson (2017) present.

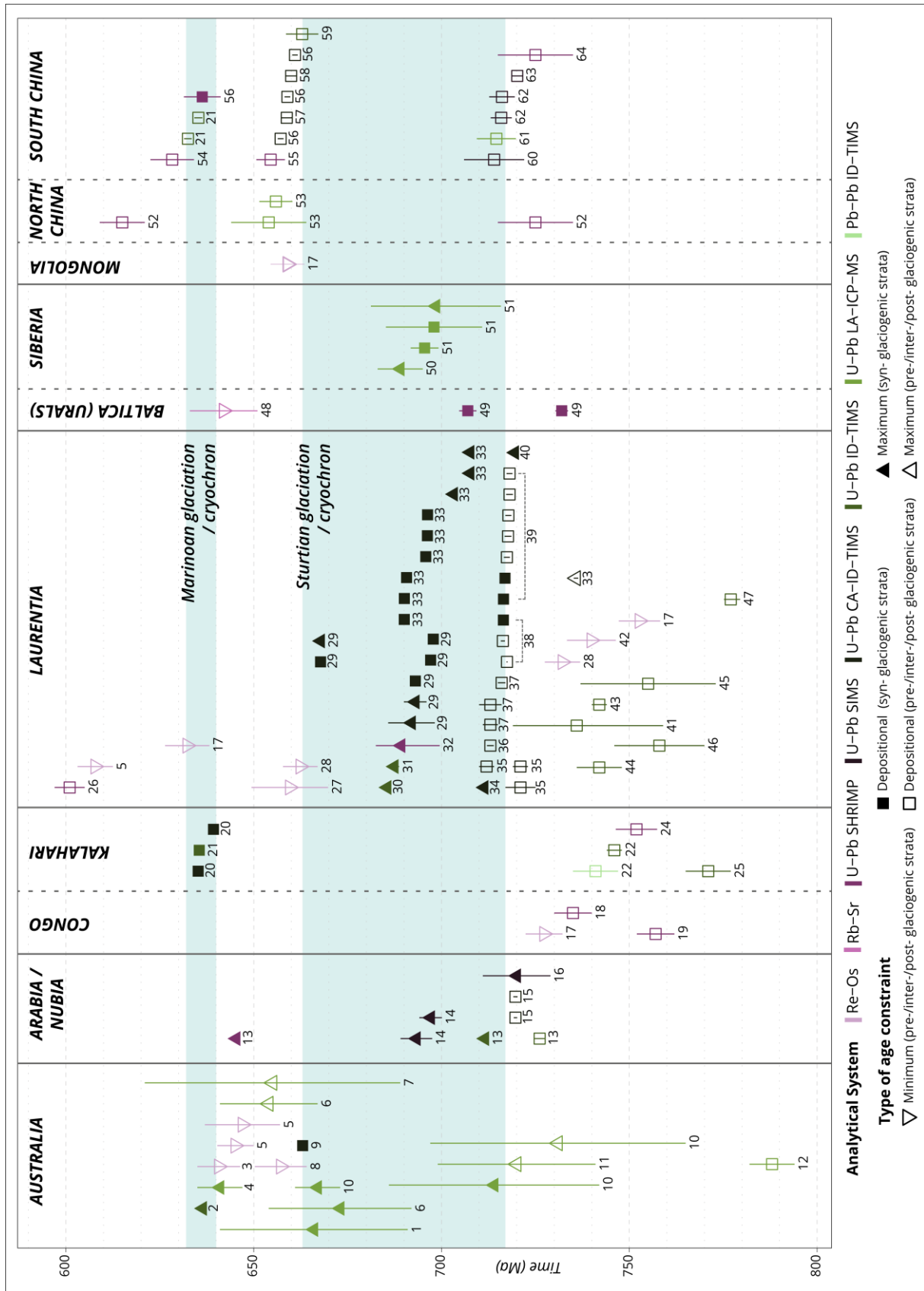
666 Additionally, data from our study refute the Le Heron et al. (2020) suggestion of a short,
667 2.4 million year, *Sturtian* glacial, 659.6 ± 10.2 Ma to 657.2 ± 5.4 Ma, based on Re-Os
668 ages from the Aralka Formation (Kendall et al. 2006), and Ballachulish Slate (Rooney et
669 al. 2011), as the Australian *Sturtian* deposits are now constrained to be older than this
670 proposed interval.

671 Considering the above, we disagree with the notion Le Heron et al. (2020) make that the
672 use of *Sturtian* to refer to a globally distributed glaciation can no longer be justified. The
673 available geochronology suggests that deposition of the Neoproterozoic glaciogenic
674 rocks, in at least, Australia (Keeman et al. 2020; Lloyd et al. 2020), Arabia/Nubia
675 (MacLennan et al. 2018; Park et al. 2019), Laurentia (Isakson 2017; Macdonald et al.
676 2018), South China (Lan et al. 2020; Rooney et al. 2020; Song et al. 2017; Wang et al.
677 2019), and Siberia (Rud`ko et al. 2020) occurred globally within the c. 717–665 Ma

678 interval. This certainly doesn't discount the possibility of different time for the onset of
679 glaciation, or the presence of glacial advance and retreats. Final deglaciation appears to
680 be relatively synchronous globally at c. 665 Ma [Figure 10]. However, it must be noted,
681 that while Figure 10 and the equivalent diagram in Le Heron et al. (2020) provide brevity
682 for visualisation and assessment of the expanding global geochronologic datasets for
683 the Cryogenian, they lack detailed stratigraphic context and detailed methodology. This
684 is an unavoidable limitation of this style of diagram, with size, legibility, and accessibility
685 (e.g, Crameri et al. 2020) all contributing to this. The ideal, entirely accurate
686 representation of all this data globally, would be detailed stratigraphic logs of each
687 section with accompanying regional correlations and detailed geochronology
688 methodology. At present, in some regions this information is either unavailable, or
689 otherwise unreliable/limited. It would also require significant space and would be best
690 attempted in a global review. To highlight this point though, the apparent diachroneity of
691 glacial onset present in Laurentia may in part be a result of complexity in zircons (post
692 crystallisation Pb loss) that may be slightly older than current determinations suggest,
693 as hinted at by Isakson (2017), and that these dates are from within glaciogenic strata
694 with both over, and underlying portions of glaciogenic strata. The volcanogenic strata
695 and corresponding dates really provide a maximum age for the mid- to upper portions of
696 the glaciogenic formation and do not preclude slightly earlier initiation. Eyster et al.
697 (2018) also highlights how this type of ambiguous interpretation was used to argue for a
698 diachroneity of onset (Baldwin et al. 2016).

699 Careful scrutiny of geochronologic data, particularly detrital zircon data, as a maximum
700 age constraint rather than as depositional age, stratigraphic position and relationships,
701 and carefully considering the limitations of geochronologic studies and methods, is
702 essential as misinterpretations of either can lead to spurious conclusions e.g., “the
703 Kaigas Formation was previously miscorrelated with glaciogenic strata of the Numees
704 Formation” (Rooney et al. 2015).

705



706

707

708

Figure caption on next page.

709 Figure 10 – Compilation of global geochronologic data for *Sturtian* and *Marinoan glaciations*. Data sources: **AUSTRALIA:** (1)
710 This study; (2) Calver et al. (2013); (3) Kendall et al. (2009); (4) Rose et al. (2013); (5) Kendall et al. (2004); (6) Lloyd et al.
711 (2020); (7) Ireland et al. (1998); (8) Kendall et al. (2006); (9) Cox et al. (2018b); (10) Keeman et al. (2020); (11) van der Wolff
712 (2020); (12) Armistead et al. (2020). **ARABIA/NUBIA:** (13) Bowring et al. (2007); (14) Abd El-Rahman et al. (2020); (15)
713 MacLennan et al. (2018); (16) Li et al. (2018). **CONGO:** (17) Rooney et al. (2015); (18) Key et al. (2001); (19) Nascimento et al.
714 (2016). **KALAHARI:** (20) Prave et al. (2016); (21) Schmitz (2012); (22) Frimmel et al. (1996); (23) Hoffman et al. (1996); (24)
715 (Borg et al. 2003); (25) Frimmel et al. (2001). **LAURENTIA:** (5) Kendall et al. (2004); (17) Rooney et al. (2015); (26) Dempster
716 et al. 2002); (27) Rooney et al. (2011); (28) Rooney et al. (2014); (29) Isakson (2017); (30) Keeley et al. (2013); (31) Condon
717 and Bowring (2011); (32) Lund et al. (2003); (33) Eyster et al. (2018); (34) Baldwin et al. (2016); (35) Denyszyn et al. (2009b);
718 (36) Cox et al. (2018a); (37) Denyszyn et al. (2009a); (38) Macdonald et al. (2010); (39) Macdonald et al. (2018); (40) Cox et
719 al. (2015); (41) McDonough and Parrish (1991); (42) Strauss et al. (2014); (43) Fetter and Goldberg (1995); (44) Karlstrom et
720 al. (2000); (45) Ross and Villeneuve (1997); (46) Aleinikoff et al. 1995); (47) Jefferson and Parrish (1989). **BALTICA (URALS):**
721 (48) Zaitseva et al. (2019); (49) Krasnobaeov et al. (2019). **SIBERIA:** (50) Kochnev et al. (2015); (51) Rud`ko et al. 2020).
722 **MONGOLIA:** (17) Rooney et al. (2015). **NORTH CHINA:** (52) Xu et al. (2009); (53) He et al. (2014). **SOUTH CHINA:** (21)
723 Schmitz (2012); (54) Chongyu et al. (2005); (55) Zhang, S et al. (2005); (56) Rooney et al. (2020); (57) Zhou, C et al. (2019);
724 (58) Zhou, C-M et al. (2020); (59) Zhou, C et al. (2004); (60) Lan et al. (2015); (61) Song et al. (2017); (62) Lan et al. (2014);
725 (63) Lan et al. (2020); (64) Zhang, Q-R et al. (2008)

726 6 Conclusions

727 This research provides an updated chronostratigraphic framework for the Yudnamutana
728 Subgroup of South Australia, i.e., the true *Sturtian glaciation*. Additionally, the
729 lithostratigraphy representing the glacial maximum of the *Sturtian glaciation* in South
730 Australia is consolidated and redefined as the Sturt Formation.

731 Key findings of this research are:

- 732 • An MDA for the (upper) Sturt Formation in the Copley area of 666 ± 25 Ma,
733 providing independent support for MDAs obtained by Keeman et al. (2020) and
734 Lloyd et al. (2020) elsewhere in the Adelaide Superbasin.
- 735 • Broadly equivalent detrital zircon spectra of all samples, with local variation, and
736 similarity to underlying Burra and Callanna Group rocks suggests recycling of
737 underlying stratigraphy and sourcing of detritus from local basement rocks.
- 738 • Detrital zircon spectra provide support to lithostratigraphic correlation of
739 Yancowinna Subgroup (New South Wales) to the Yudnamutana Subgroup (South
740 Australia).
- 741 • Support for the continued use of *Sturtian glaciation* or *cryochron* globally.

742 Funding

743 The Geological Survey of South Australia and the MinEx CRC funded this research. This
744 research was supported by an Australian Government Research Training Program (RTP)
745 Scholarship awarded to JCL.

746 Data Availability

747 Complete data for this publication are freely available for download from figshare at the
748 following links. These datasets contain all the U–Pb geochronology data, trace element
749 data, and basic sample metadata.

750 Zircon and NIST standards data for all analytical sessions:

751 <https://doi.org/10.6084/m9.figshare.18131432> (Lloyd et al. 2022b)

752 Yudnamutana Subgroup detrital zircon data (this study):

753 <https://doi.org/10.6084/m9.figshare.19181144> (Lloyd et al. 2022d)

754 Zircon CL images: <https://doi.org/10.6084/m9.figshare.19181024>

755 Code Availability

756 R code used to generate the zircon geochemistry plots is available on GitHub at

757 <https://github.com/jarredclloyd/zircon-trace-element-plots>

758 CRediT author statement

759 **Jarred C. Lloyd:** Conceptualisation, investigation, writing - original draft, writing -
760 review & editing, methodology, formal analysis, data curation, visualisation. **Wolfgang**
761 **V. Preiss:** Investigation, writing – review and editing. **Alan S. Collins:**
762 Conceptualisation, funding acquisition, supervision, investigation, writing - review &
763 editing. **Georgina M. Virgo:** Investigation, writing – review and editing. **Morgan L.**
764 **Blades:** Investigation, writing - review & editing. **Sarah E. Gilbert:** Formal analysis,
765 methodology, investigation, writing - review & editing. **Kathryn J. Amos:**
766 Conceptualisation, supervision, writing - review & editing.

767 Acknowledgements

768 We acknowledge the Adnyamathanha, Arabana, Banggarla, Kurna, Kokatha, Kuyani,
769 Ngadjuri and Nukunu Peoples as the Traditional Owners and Custodians of the land on
770 which this research is conducted. We acknowledge and respect their deep feelings of
771 attachment and spiritual relationship to Country, and that their cultural and heritage
772 beliefs are still as important to the living people today.

773 The authors acknowledge the instruments and scientific and technical assistance of
774 Microscopy Australia at Adelaide Microscopy, The University of Adelaide, a facility that is
775 funded by the University, and State and Federal Governments. Particular thanks to Aoife
776 McFadden for their assistance with SEM-CL imaging.

777 We also thank James Nankivell (University of Adelaide) for their assistance with
778 fieldwork, and the Geological Survey of South Australia and MinEx CRC for funding the
779 research. Chris Folkes (Geological Survey of New South Wales) and John Greenfield
780 (formerly GSNSW) are thanked for their expertise on the New South Wales sequences.

781 This work is conducted with the relevant permissions and scientific permits from the
782 relevant stakeholders. This publication forms MinEx CRC output #XXXX

783 References

- 784 Abd El-Rahman, Y, Gutzmer, J, Li, X-H, Seifert, T, Li, C-F, Ling, X-X & Li, J 2020, 'Not all Neoproterozoic
785 iron formations are glaciogenic: Sturtian-aged non-Rapitan exhalative iron formations from
786 the Arabian–Nubian Shield', *Mineralium Deposita*, vol. 55, no. 3, pp. 577-596.
787 doi:10.1007/s00126-019-00898-0.
- 788 Aleinikoff, JN, Zartman, RE, Walter, M, Rankin, DW, Lyttle, PT & Burton, WC 1995, 'U-Pb ages of
789 metarhyolites of the Catoctin and Mount Rogers formations, Central and Southern
790 Appalachians; evidence for two pulses of Iapetan rifting', *American Journal of Science*, vol.
791 295, no. 4, p. 428. doi:10.2475/ajs.295.4.428.
- 792 Ali, DO, Spencer, AM, Fairchild, IJ, Chew, KJ, Anderton, R, Levell, BK, Hambrey, MJ, Dove, D & Le
793 Heron, DP 2018, 'Indicators of relative completeness of the glacial record of the Port Askaig
794 Formation, Garvellach Islands, Scotland', *Precambrian Research*, vol. 319, pp. 65-78.
795 doi:10.1016/j.precamres.2017.12.005.
- 796 Allen, PA & Etienne, JL 2008, 'Sedimentary challenge to Snowball Earth', *Nature Geoscience*, vol. 1,
797 no. 12, pp. 817-825. doi:10.1038/ngeo355.
- 798 Ambrose, GJ, Flint, RB & Webb, AW 1981, *Precambrian and Palaeozoic Geology of the Peake and
799 Denison Ranges*, Bulletin, 50, Geological Survey of South Australia, Adelaide, South Australia.
- 800 Anenburg, M 2020, 'Rare earth mineral diversity controlled by REE pattern shapes', *Mineralogical
801 Magazine*, vol. 84, no. 5, pp. 629-639. doi:10.1180/mgm.2020.70.
- 802 Anenburg, M & Williams, MJ 2021, 'Quantifying the Tetrad Effect, Shape Components, and Ce–Eu–Gd
803 Anomalies in Rare Earth Element Patterns', *Mathematical Geosciences*. doi:10.1007/s11004-
804 021-09959-5.
- 805 Armistead, SE, Collins, AS, Buckman, S & Atkins, R 2020, 'Age and geochemistry of the Boucaut
806 Volcanics in the Neoproterozoic Adelaide Rift Complex, South Australia', *Australian Journal of
807 Earth Sciences*, pp. 1-10. doi:10.1080/08120099.2021.1840435.
- 808 Arnaud, E, Halverson, GP & Shields-Zhou, GA (eds) 2011, *The Geological Record of Neoproterozoic
809 Glaciations*, Memoirs, 36, Geological Society, London.
- 810 Baldwin, GJ, Turner, EC & Kamber, BS 2016, 'Tectonic controls on distribution and stratigraphy of the
811 Cryogenian Rapitan iron formation, northwestern Canada', *Precambrian Research*, vol. 278,
812 pp. 303-322. doi:10.1016/j.precamres.2016.03.014.
- 813 Barovich, KM & Hand, M 2008, 'Tectonic setting and provenance of the Paleoproterozoic Willyama
814 Supergroup, Curnamona Province, Australia: Geochemical and Nd isotopic constraints on
815 contrasting source terrain components', *Precambrian Research*, vol. 166, no. 1, pp. 318-337.
816 doi:10.1016/j.precamres.2007.06.024.
- 817 Belousova, EA, Reid, AJ, Griffin, WL & O'Reilly, SY 2009, 'Rejuvenation vs. recycling of Archean crust
818 in the Gawler Craton, South Australia: Evidence from U–Pb and Hf isotopes in detrital zircon',
819 *Lithos*, vol. 113, no. 3-4, pp. 570-582. doi:10.1016/j.lithos.2009.06.028.
- 820 Belperio, AP 1973, 'The stratigraphy and facies of the Late Precambrian Lower Glacial sequence, Mt
821 Painter, South Australia', Department of Geology, Honours Thesis, Bachelor of Science
822 (Honours), University of Adelaide, Adelaide, South Australia.
- 823 Borg, G, Kärner, K, Buxton, M, Armstrong, R & Merwe, SWvd 2003, 'Geology of the Skorpion
824 Supergene Zinc Deposit, Southern Namibia', *Economic Geology*, vol. 98, no. 4, pp. 749-771.
825 doi:10.2113/gsecongeo.98.4.749.
- 826 Bowring, SA, Grotzinger, JP, Condon, DJ, Ramezani, J, Newall, MJ & Allen, PA 2007, 'Geochronologic
827 constraints on the chronostratigraphic framework of the Neoproterozoic Huqf Supergroup,
828 Sultanate of Oman', *American Journal of Science*, vol. 307, no. 10, pp. 1097-1145.
829 doi:10.2475/10.2007.01.
- 830 Brocks, JJ 2018, 'The transition from a cyanobacterial to algal world and the emergence of animals',
831 *Emerging Topics in Life Sciences*, vol. 2, no. 2, pp. 181-190. doi:10.1042/etls20180039.

- 832 Brocks, JJ, Jarrett, AJM, Sirantoine, E, Hallmann, C, Hoshino, Y & Liyanage, T 2017, 'The rise of algae
833 in Cryogenian oceans and the emergence of animals', *Nature*, vol. 548, no. 7669, pp. 578-
834 581. doi:10.1038/nature23457.
- 835 Callen, RA 1990, *Curnamona*, 1:250 000 Geological Series—Explanatory Notes, Department of Mines
836 and Energy, Adelaide, South Australia.
- 837 Calver, CR, Crowley, JL, Wingate, MTD, Evans, DAD, Raub, TD & Schmitz, MD 2013, 'Globally
838 synchronous Marinoan deglaciation indicated by U-Pb geochronology of the Cottons Breccia,
839 Tasmania, Australia', *Geology*, vol. 41, no. 10, pp. 1127-1130. doi:10.1130/g34568.1.
- 840 Chongyu, Y, Feng, T, Liu, Y, Gao, L, Yang, Z, Wang, Z, Liu 刘鹏举, P, Xing, YZ & Song, B 2005, 'New U-
841 Pb zircon ages from the Ediacaran (Sinian) System in the Yangtze Gorges: Constraint on the
842 age of Miaohe biota and Marinoan glaciation', *Geological Bulletin of China*, vol. 24, pp. 393-
843 400.
- 844 Coats, RP & Forbes, BG 1977, 'Evidence for two Sturtian Glaciations in South Australia', *Quarterly
845 Geological Notes*, vol. 64, pp. 19-20.
846 [https://sarigbasis.pir.sa.gov.au/WebtopEw/ws/samref/sarig1/wci/Record?r=0&m=1&w=cat
847 no=2041398](https://sarigbasis.pir.sa.gov.au/WebtopEw/ws/samref/sarig1/wci/Record?r=0&m=1&w=catno=2041398).
- 848 Coats, RP & Preiss, WV 1987, 'Stratigraphy of the Umberatana Group', in WV Preiss (ed.), *Adelaide
849 Geosyncline—late Proterozoic stratigraphy, sedimentation, palaeontology and tectonics*,
850 Geological Survey of South Australia, Adelaide, South Australia, pp. 125-211.
- 851 Condon, DJ & Bowring, SA 2011, 'A user's guide to Neoproterozoic geochronology', in E Arnaud, GP
852 Halverson & GA Shields-Zhou (eds), *The Geological Record of Neoproterozoic Glaciations*,
853 Geological Society, London, pp. 135-149.
- 854 Conor, CHH & Preiss, WV 2008, 'Understanding the 1720–1640Ma Palaeoproterozoic Willyama
855 Supergroup, Curnamona Province, Southeastern Australia: Implications for tectonics, basin
856 evolution and ore genesis', *Precambrian Research*, vol. 166, no. 1, pp. 297-317.
857 doi:10.1016/j.precamres.2007.08.020.
- 858 Conor, CHH & Preiss, WV 2019, 'Cryogenian glaciomarine megaclasts of the MacDonald Corridor,
859 Bimbowrie Conservation Park, Olary Region, South Australia', *Australian Journal of Earth
860 Sciences*, vol. 67, no. 6, pp. 857-872. doi:10.1080/08120099.2018.1553206.
- 861 Cooper, BJ 2010, 'Snowball Earth': The Early Contribution from South Australia', *Earth Sciences
862 History*, vol. 29, no. 1, pp. 121-145. doi:10.17704/eshi.29.1.j8874825610u68w5.
- 863 Cooper, PF 1973, 'Striated Pebbles from the Late Precambrian Adelaidean', *Quarterly Notes -
864 Geological Survey of New South Wales*, vol. 11, pp. 13-15.
- 865 Cooper, PF & Tuckwell, KD 1971, 'The upper Precambrian Adelaidean of the Broken Hill area—a new
866 subdivision', *Quarterly Notes - Geological Survey of New South Wales*, vol. 3, pp. 8-16.
- 867 Cooper, PF, Tuckwell, KD, Gilligan, LB & Meares, RMD 1974, *Geology of the Torrawangee and Fowlers
868 Gap 1:100,000 Sheets*, Geological Survey of New South Wales, Department of Mines, Sydney,
869 New South Wales.
- 870 Counts, JW 2017, *The Adelaide Rift Complex in the Flinders Ranges: geologic history, past
871 investigations and relevant analogues*, Report Book, no. 2017/00016, Geological Survey of
872 South Australia, Department of Premier and Cabinet, Adelaide, South Australia,
873 <[https://sarigbasis.pir.sa.gov.au/WebtopEw/ws/samref/sarig1/wcir/Record?r=0&m=1&w=ca
874 tno=2039731](https://sarigbasis.pir.sa.gov.au/WebtopEw/ws/samref/sarig1/wcir/Record?r=0&m=1&w=catno=2039731)>.
- 875 Cowley, WM 2020, 'Geological setting of exceptional geological features of the Flinders Ranges',
876 *Australian Journal of Earth Sciences*, pp. 1-23. doi:10.1080/08120099.2020.1748109.
- 877 Cox, GM, Halverson, GP, Denyszyn, S, Foden, J & Macdonald, FA 2018a, 'Cryogenian magmatism
878 along the north-western margin of Laurentia: Plume or rift?', *Precambrian Research*, vol. 319,
879 pp. 144-157. doi:10.1016/j.precamres.2017.09.025.
- 880 Cox, GM, Halverson, GP, Minarik, WG, Le Heron, DP, Macdonald, FA, Bellefroid, EJ & Strauss, JV 2013,
881 'Neoproterozoic iron formation: An evaluation of its temporal, environmental and tectonic
882 significance', *Chemical Geology*, vol. 362, pp. 232-249. doi:10.1016/j.chemgeo.2013.08.002.

- 883 Cox, GM, Isakson, V, Hoffman, PF, Gernon, TM, Schmitz, MD, Shahin, S, Collins, AS, Preiss, WV,
884 Blades, ML, Mitchell, RN & Nordsvan, A 2018b, 'South Australian U-Pb zircon (CA-ID-TIMS)
885 age supports globally synchronous Sturtian deglaciation', *Precambrian Research*, vol. 315,
886 pp. 257-263. doi:10.1016/j.precamres.2018.07.007.
- 887 Cox, GM, Strauss, JV, Halverson, GP, Schmitz, MD, McClelland, WC, Stevenson, RS & Macdonald, FA
888 2015, 'Kikiktat volcanics of Arctic Alaska—Melting of harzburgitic mantle associated with the
889 Franklin large igneous province', *Lithosphere*, vol. 7, no. 3, pp. 275-295. doi:10.1130/l435.1.
- 890 Cramer, F, Shephard, GE & Heron, PJ 2020, 'The misuse of colour in science communication', *Nat*
891 *Commun*, vol. 11, no. 1, p. 5444. doi:10.1038/s41467-020-19160-7.
- 892 Dalgarno, CR & Johnson, JE 1966, *Parachilna map sheet SH54-13*, 1st edn, Geological Atlas of South
893 Australia, 1:250 000 series, Geological Survey of South Australia, Adelaide, South Australia.
- 894 David, TWE 1906, 'Australis: les conditions du climat aux époques géologiques', in *10th*
895 *International Geological Congress*, Mexico.
- 896 Dempster, TJ, Rogers, G, Tanner, PWG, Bluck, BJ, Muir, RJ, Redwood, SD, Ireland, TR & Paterson, BA
897 2002, 'Timing of deposition, orogenesis and glaciation within the Dalradian rocks of Scotland:
898 constraints from U–Pb zircon ages', *Journal of the Geological Society*, vol. 159, no. 1, pp. 83-
899 94. doi:10.1144/0016-764901061.
- 900 Denyszyn, SW, Davis, DW & Halls, HC 2009a, 'Paleomagnetism and U–Pb geochronology of the
901 Clarence Head dykes, Arctic Canada: orthogonal emplacement of mafic dykes in a large
902 igneous province', *Canadian Journal of Earth Sciences*, vol. 46, no. 3, pp. 155-167.
903 doi:10.1139/E09-011.
- 904 Denyszyn, SW, Halls, HC, Davis, DW & Evans, DAD 2009b, 'Paleomagnetism and U–Pb geochronology
905 of Franklin dykes in High Arctic Canada and Greenland: a revised age and paleomagnetic pole
906 constraining block rotations in the Nares Strait region', *Canadian Journal of Earth Sciences*,
907 vol. 46, no. 9, pp. 689-705. doi:10.1139/E09-042.
- 908 Drexel, JF & Preiss, WV (eds) 1995, *The geology of South Australia*, vol. 2, The Phanerozoic, Bulletin,
909 54, Geological Survey of South Australia, South Australia.
- 910 Dröllner, M, Barham, M, Kirkland, CL & Ware, B 2021, 'Every zircon deserves a date: selection bias in
911 detrital geochronology', *Geological Magazine*, vol. 158, no. 6, pp. 1135-1142.
912 doi:10.1017/s0016756821000145.
- 913 Dunn, PR, Thomson, BP & Rankama, K 1971, 'Late Pre-Cambrian Glaciation in Australia as a
914 Stratigraphic Boundary', *Nature*, vol. 231, no. 5304, pp. 498-502. doi:10.1038/231498a0.
- 915 Dyson, IA 1996, 'Stratigraphy of the Burra and Umberatana Groups in the Willippa Anticline, central
916 Flinders Ranges', *Quarterly Geological Notes*, vol. 129, pp. 10-26.
- 917 Dyson, IA 2004, 'Geology of the eastern Willouran Ranges - evidence for earliest onset of salt
918 tectonics in the Adelaide Geosyncline', *MESA Journal*, vol. 35, pp. 46-56.
919 [https://sarigbasis.pir.sa.gov.au/WebtopEw/ws/samref/sarig1/wci/Record?r=0&m=1&w=catn](https://sarigbasis.pir.sa.gov.au/WebtopEw/ws/samref/sarig1/wci/Record?r=0&m=1&w=catno=2023965)
920 [o=2023965](https://sarigbasis.pir.sa.gov.au/WebtopEw/ws/samref/sarig1/wci/Record?r=0&m=1&w=catno=2023965).
- 921 Edgoose, CJ 2013, 'Chapter 23: Amadeus Basin', in M Ahmad & TJ Munson (eds), *Geology and*
922 *mineral resources of the Northern Territory*, Northern Territory Geological Survey, Northern
923 Territory.
- 924 Eyles, N & Januszczak, N 2004, 'Zipper-rift': a tectonic model for Neoproterozoic glaciations during
925 the breakup of Rodinia after 750 Ma', *Earth-Science Reviews*, vol. 65, no. 1-2, pp. 1-73.
926 doi:10.1016/s0012-8252(03)00080-1.
- 927 Eyster, A, Ferri, F, Schmitz, MD & Macdonald, FA 2018, 'One diamictite and two rifts: Stratigraphy and
928 geochronology of the Gataga Mountain of northern British Columbia', *American Journal of*
929 *Science*, vol. 318, no. 2, pp. 167-207. doi:10.2475/02.2018.1.
- 930 Fairchild, IJ & Kennedy, MJ 2007, 'Neoproterozoic glaciation in the Earth System', *Journal of the*
931 *Geological Society*, vol. 164, no. 5, pp. 895-921. doi:10.1144/0016-76492006-191.

932 Fairchild, IJ, Spencer, AM, Ali, DO, Anderson, RP, Anderton, R, Boomer, I, Dove, D, Evans, JD,
933 Hambrey, MJ, Howe, J, Sawaki, Y, Shields, GA, Skelton, A, Tucker, ME, Wang, Z & Zhou, Y
934 2018, 'Tonian-Cryogenian boundary sections of Argyll, Scotland', *Precambrian Research*, vol.
935 319, pp. 37-64. doi:10.1016/j.precamres.2017.09.020.

936 Fanning, CM & Link, PK 2004, 'U-Pb SHRIMP ages of Neoproterozoic (Sturtian) glaciogenic Pocatello
937 Formation, southeastern Idaho', *Geology*, vol. 32, no. 10, pp. 881-884.
938 doi:10.1130/G20609.1.

939 Fanning, CM & Link, PK 2006, 'Constraints on the timing of the Sturtian Glaciation from Southern
940 Australia; IE for the true Sturtian', in *2006 Philadelphia Annual Meeting*, vol. 7, Geological
941 Society of America, Pennsylvania, p. 115.

942 Fanning, CM & Link, PK 2008, 'Age constraints for the Sturtian Glaciation; data from the Adelaide
943 Geosyncline, South Australia and Pocatello Formation, Idaho, USA', in SJ Gallagher & MW
944 Wallace (eds), *Neoproterozoic extreme climates and the origin of early metazoan life, Selwyn
945 Symposium of the GSA Victoria Division*, Geological Society of Australia, The University of
946 Melbourne, vol. 91, pp. 57-62.

947 Fanning, CM, Reid, AJ & Teale, GS 2007, *A geochronological framework for the Gawler Craton, South
948 Australia*, Bulletin, 55, Geological Survey of South Australia, Adelaide, South Australia.

949 Fergusson, CL, Henderson, RA, Fanning, CM & Withnall, IW 2007, 'Detrital zircon ages in
950 Neoproterozoic to Ordovician siliciclastic rocks, northeastern Australia: implications for the
951 tectonic history of the East Gondwana continental margin', *Journal of the Geological Society*,
952 vol. 164, no. 1, pp. 215-225. doi:10.1144/0016-76492005-136.

953 Fetter, AH & Goldberg, SA 1995, 'Age and Geochemical Characteristics of Bimodal Magmatism in the
954 Neoproterozoic Grandfather Mountain Rift Basin', *The Journal of Geology*, vol. 103, no. 3, pp.
955 313-326. doi:10.1086/629749.

956 Fioretti, AM, Black, LP, Foden, J & Visonà, D 2005, 'Grenville-age magmatism at the South Tasman
957 Rise (Australia): A new piercing point for the reconstruction of Rodinia', *Geology*, vol. 33, no.
958 10, pp. 769-772. doi:10.1130/G21671.1.

959 Fitzherbert, JA & Downes, PM 2015, 'A concise geological history of the Broken Hill region', *Quarterly
960 Notes - Geological Survey of New South Wales*, vol. 143, no. 2, pp. 29-43.

961 Foden, JD, Elburg, MA, Dougherty-Page, J & Burt, A 2006, 'The timing and duration of the
962 Delamerian orogeny: Correlation with the Ross Orogen and implications for Gondwana
963 assembly', *Journal of Geology*, vol. 114, no. 2, pp. 189-210. doi:10.1086/499570.

964 Foden, JD, Elburg, MA, Turner, S, Clark, C, Blades, ML, Cox, G, Collins, AS, Wolff, K & George, C 2020,
965 'Cambro-Ordovician magmatism in the Delamerian orogeny: Implications for tectonic
966 development of the southern Gondwanan margin', *Gondwana Research*.
967 doi:10.1016/j.gr.2019.12.006.

968 Forbes, BG 1971, *Parachilna, 1:250 000 Geological Series—Explanatory Notes*, Department of Mines
969 South Australia, Adelaide, South Australia.

970 Forbes, BG & Cooper, RS 1976, 'The Pualco Tillite of the Olary Region, South Australia', *Quarterly
971 Geological Notes*, vol. 60, pp. 2-5.

972 Fraser, GL, McAvaney, S, Neumann, NL, Szpunar, M & Reid, A 2010, 'Discovery of early Mesoarchean
973 crust in the eastern Gawler Craton, South Australia', *Precambrian Research*, vol. 179, no. 1,
974 pp. 1-21. doi:10.1016/j.precamres.2010.02.008.

975 Fraser, GL & Neumann, NL 2010, *New SHRIMP U-Pb Zircon Ages from the Gawler Craton and
976 Curnamona Province, South Australia, 2008 - 2010*, Record, no. 2010/16, Geoscience
977 Australia, Canberra, <<http://pid.geoscience.gov.au/dataset/ga/70348>>.

978 Frimmel, HE, Klötzli, US & Siegfried, PR 1996, 'New Pb-Pb Single Zircon Age Constraints on the
979 Timing of Neoproterozoic Glaciation and Continental Break-up in Namibia', *The Journal of
980 Geology*, vol. 104, pp. 459-469. doi:10.1086/629839.

981 Frimmel, HE, Zartman, RE & Späth, A 2001, 'The Richtersveld Igneous Complex, South Africa: U-Pb
982 Zircon and Geochemical Evidence for the Beginning of Neoproterozoic Continental Breakup',
983 *The Journal of Geology*, vol. 109, pp. 493-508. doi:10.1086/320795.
984 Gehrels, GE, Valencia, VA & Ruiz, J 2008, 'Enhanced precision, accuracy, efficiency, and spatial
985 resolution of U-Pb ages by laser ablation-multicollector-inductively coupled plasma-mass
986 spectrometry', *Geochemistry, Geophysics, Geosystems*, vol. 9, no. 3.
987 doi:10.1029/2007gc001805.
988 Gradstein, FM, Ogg, JG & Smith, AG (eds) 2005, *A Geologic Time Scale 2004*, Cambridge University
989 Press, Cambridge.
990 Grimes, CB, John, BE, Kelemen, PB, Mazdab, FK, Wooden, JL, Cheadle, MJ, Hanghøj, K & Schwartz, JJ
991 2007, 'Trace element chemistry of zircons from oceanic crust: A method for distinguishing
992 detrital zircon provenance', *Geology*, vol. 35, no. 7, pp. 643-646. doi:10.1130/G23603A.1.
993 Grimes, CB, Wooden, JL, Cheadle, MJ & John, BE 2015, "'Fingerprinting" tectono-magmatic
994 provenance using trace elements in igneous zircon', *Contributions to Mineralogy and
995 Petrology*, vol. 170, no. 5, p. 46. doi:10.1007/s00410-015-1199-3.
996 Halverson, GP, Hurtgen, MT, Porter, SM & Collins, AS 2009, 'Neoproterozoic-Cambrian
997 Biogeochemical Evolution', in C Gaucher, AN Sial, HE Frimmel & GP Halverson (eds),
998 *Developments in Precambrian Geology*, vol. 16, Elsevier, pp. 351-365.
999 Halverson, GP, Kunzmann, M, Strauss, JV & Maloof, AC 2017, 'The Tonian-Cryogenian transition in
1000 Northeastern Svalbard', *Precambrian Research*, vol. 319, pp. 79-95.
1001 doi:10.1016/j.precamres.2017.12.010.
1002 Halverson, GP, Porter, SM & Gibson, TM 2018, 'Dating the late Proterozoic stratigraphic record',
1003 *Emerging Topics in Life Sciences*, vol. 2, no. 2, pp. 137-147. doi:10.1042/etls20170167.
1004 He, J, Zhu, W & Ge, R 2014, 'New age constraints on Neoproterozoic diamictites in Kuruktag, NW
1005 China and Precambrian crustal evolution of the Tarim Craton', *Precambrian Research*, vol.
1006 241, pp. 44-60. doi:10.1016/j.precamres.2013.11.005.
1007 Hoffman, PF 2011, 'A history of Neoproterozoic glacial geology, 1871-1997', in E Arnaud, GP
1008 Halverson & GA Shields-Zhou (eds), *The Geological Record of Neoproterozoic Glaciations*,
1009 Geological Society, London, pp. 17-37.
1010 Hoffman, PF, Abbot, DS, Ashkenazy, Y, Benn, DI, Brocks, JJ, Cohen, PA, Cox, GM, Creveling, JR,
1011 Donnadieu, Y, Erwin, DH, Fairchild, IJ, Ferreira, D, Goodman, JC, Halverson, GP, Jansen, MF,
1012 Le Hir, G, Love, GD, Macdonald, FA, Maloof, AC, Partin, CA, Ramstein, G, Rose, BEJ, Rose, CV,
1013 Sadler, PM, Tziperman, E, Voigt, A & Warren, SG 2017a, 'Snowball Earth climate dynamics
1014 and Cryogenian geology-geobiology', *Science Advances*, vol. 3, no. 11, p. e1600983.
1015 doi:10.1126/sciadv.1600983.
1016 Hoffman, PF & Halverson, GP 2011, 'Neoproterozoic glacial record in the Mackenzie Mountains,
1017 northern Canadian Cordillera', in E Arnaud, GP Halverson & GA Shields-Zhou (eds), *The
1018 Geological Record of Neoproterozoic Glaciations*, Geological Society, London, pp. 397-412.
1019 Hoffman, PF, Halverson, GP, Schrag, DP, Higgins, JA, Domack, EW, Macdonald, FA, Pruss, SB, Blättler,
1020 CL, Crockford, PW, Hodgkin, EB, Bellefroid, EJ, Johnson, BW, Hodgskiss, MSW, Lamothe, KG,
1021 LoBianco, SJC, Busch, JF, Howes, BJ, Greenman, JW & Nelson, LL 2021, 'Snowballs in Africa:
1022 sectioning a long-lived Neoproterozoic carbonate platform and its bathyal foreslope (NW
1023 Namibia)', *Earth-Science Reviews*, vol. 219. doi:10.1016/j.earscirev.2021.103616.
1024 Hoffman, PF, Hawkins, D, Isachsen, C & Bowring, SA 1996, 'Precise U-Pb zircon ages for early
1025 Damaran magmatism in the Summas Mountains and Welwitschia Inlier, northern Damara
1026 belt, Namibia', *Communications of the geological survey of Namibia*, vol. 11, pp. 47-52.
1027 Hoffman, PF, Kaufman, AJ, Halverson, GP & Schrag, DP 1998, 'A Neoproterozoic Snowball Earth',
1028 *Science*, vol. 281, no. 5381, p. 1342. doi:10.1126/science.281.5381.1342.

1029 Hoffman, PF, Lamothe, KG, LoBianco, SJC, Hodgskiss, MSW, Bellefroid, EJ, Johnson, BW, Hodgkin, EB
1030 & Halverson, GP 2017b, 'Sedimentary depocenters on Snowball Earth: Case studies from the
1031 Sturtian Chuos Formation in northern Namibia', *Geosphere*, vol. 13, no. 3, pp. 811-837.
1032 doi:10.1130/ges01457.1.

1033 Hoffman, PF & Schrag, DP 2002, 'The snowball Earth hypothesis: testing the limits of global change',
1034 *Terra Nova*, vol. 14, no. 3, pp. 129-155. doi:10.1046/j.1365-3121.2002.00408.x.

1035 Horstwood, MSA, Košler, J, Gehrels, GE, Jackson, SE, McLean, NM, Paton, C, Pearson, NJ, Sircombe,
1036 KN, Sylvester, P, Vermeesch, P, Bowring, JF, Condon, DJ & Schoene, B 2016, 'Community-
1037 Derived Standards for LA-ICP-MS U-(Th)-Pb Geochronology - Uncertainty Propagation, Age
1038 Interpretation and Data Reporting', *Geostandards and Geoanalytical Research*, vol. 40, no. 3,
1039 pp. 311-332. doi:10.1111/j.1751-908X.2016.00379.x.

1040 Hoskin, PWO & Ireland, TR 2000, 'Rare earth element chemistry of zircon and its use as a provenance
1041 indicator', *Geology*, vol. 28, no. 7, pp. 627-630. doi:10.1130/0091-
1042 7613(2000)28<627:REECOZ>2.0.CO;2.

1043 Hoskin, PWO & Schaltegger, U 2003, 'The composition of zircon and igneous and metamorphic
1044 petrogenesis', *Reviews in Mineralogy and Geochemistry*, vol. 53, no. 1, pp. 27-62.
1045 doi:10.2113/0530027.

1046 Howchin, W 1901, 'Preliminary Note on the Existence of Glacial Beds of Cambrian Age in South
1047 Australia', *Transactions of the Royal Society of South Australia*, vol. 25, pp. 10-13.

1048 Howchin, W 1904, 'The geology of the Mount Lofty Ranges: Part I', *Transactions of the Royal Society of*
1049 *South Australia*, vol. 28, pp. 253-280.

1050 Howchin, W 1906, 'The geology of the Mount Lofty Ranges: Part II', *Transactions of the Royal Society*
1051 *of South Australia*, vol. 30, pp. 227-262.

1052 Howchin, W 1908, 'Glacial Beds of Cambrian Age in South Australia', *Quarterly Journal of the*
1053 *Geological Society*, vol. 64, no. 1-4, p. 234. doi:10.1144/GSL.JGS.1908.064.01-04.13.

1054 Howchin, W 1920, 'Past Glacial Action in Australia', in ABo Statistics (ed.), *Year Book*, vol. 13,
1055 Australian Bureau of Statistics, Australia, pp. 1133-1146.

1056 Ireland, TR, Flöttmann, T, Fanning, CM, Gibson, GM & Preiss, WV 1998, 'Development of the early
1057 Paleozoic Pacific margin of Gondwana from detrital-zircon ages across the Delamerian
1058 orogen', *Geology*, vol. 26, no. 3, pp. 243-246. doi:10.1130/0091-
1059 7613(1998)026<0243:Dotepp>2.3.Co;2.

1060 Isakson, VH 2017, 'Geochronology of the Tectonic, Stratigraphic, and Magmatic Evolution of
1061 Neoproterozoic to Early Paleozoic, North American Cordillera and Cryogenian Glaciation',
1062 Department of Geoscience, Dissertation, Doctor of Philosophy, Boise State University, Boise,
1063 Idaho, USA.

1064 Jackson, SE, Pearson, NJ, Griffin, WL & Belousova, EA 2004, 'The application of laser ablation-
1065 inductively coupled plasma-mass spectrometry to in situ U-Pb zircon geochronology',
1066 *Chemical Geology*, vol. 211, no. 1-2, pp. 47-69. doi:10.1016/j.chemgeo.2004.06.017.

1067 Jacobs, J, Elburg, MA, Läufer, A, Kleinhanns, IC, Henjes-Kunst, F, Estrada, S, Ruppel, AS, Damaske, D,
1068 Montero, P & Bea, F 2015, 'Two distinct Late Mesoproterozoic/Early Neoproterozoic
1069 basement provinces in central/eastern Dronning Maud Land, East Antarctica: The missing
1070 link, 15–21°E', *Precambrian Research*, vol. 265, pp. 249-272.
1071 doi:10.1016/j.precamres.2015.05.003.

1072 Jagodzinski, EA & Fricke, CE 2010, *Compilation of new SHRIMP U-Pb geochronological data for the*
1073 *Southern Curnamona Province, South Australia, 2010*, Report Book, no. 2010/00014,
1074 Geological Survey of South Australia, Department of Primary Industries and Resources,
1075 Adelaide, South Australia.

1076 Jagodzinski, EA & McAvaney, SO 2017, *SHRIMP U-Pb geochronology data for northern Eyre Peninsula,*
1077 *2014–2016, Report Book, no. 2016/00001, Geological Survey of South Australia, Adelaide,*
1078 *South Australia,*
1079 *<[https://sarigbasis.pir.sa.gov.au/WebtopEw/ws/samref/sarig1/wci/Record?r=0&m=1&w=cat](https://sarigbasis.pir.sa.gov.au/WebtopEw/ws/samref/sarig1/wci/Record?r=0&m=1&w=catno=2039475)*
1080 *no=2039475>.*
1081 Jagodzinski, EA, Werner, M, Curtis, S, Fabris, A, Pawley, M & Krapf, C 2020, *SHRIMP Geochronology of*
1082 *the Mt Double area, Southern Gawler Ranges margin, Report Book, no. 2020/00006,*
1083 *Geological Survey of South Australia, DfEa Mining, South Australia.*
1084 Jefferson, CW & Parrish, RR 1989, 'Late Proterozoic stratigraphy, U–Pb zircon ages, and rift tectonics,
1085 *Mackenzie Mountains, northwestern Canada', *Canadian Journal of Earth Sciences*, vol. 26, no.*
1086 *9, pp. 1784-1801. doi:10.1139/e89-151.*
1087 Jochum, KP, Weis, U, Stoll, B, Kuzmin, D, Yang, Q, Raczek, I, Jacob, DE, Stracke, A, Birbaum, K, Frick,
1088 DA, Günther, D & Enzweiler, J 2011, 'Determination of Reference Values for NIST SRM 610–
1089 617 Glasses Following ISO Guidelines', *Geostandards and Geoanalytical Research*, vol. 35,
1090 no. 4, pp. 397-429. doi:10.1111/j.1751-908X.2011.00120.x.
1091 Karlstrom, KE, Bowring, SA, Dehler, CM, Knoll, AH, Porter, SM, Marais, DJD, Weil, AB, Sharp, ZD,
1092 Geissman, JW, Elrick, MB, Timmons, JM, Crossey, LJ & Davidek, KL 2000, 'Chuar Group of the
1093 Grand Canyon: Record of breakup of Rodinia, associated change in the global carbon cycle,
1094 and ecosystem expansion by 740 Ma', *Geology*, vol. 28, no. 7, pp. 619-622.
1095 doi:10.1130/0091-7613(2000)28<619:CGOTGC>2.0.CO;2.
1096 Keeley, JA, Link, PK, Fanning, CM & Schmitz, MD 2013, 'Pre- to synglacial rift-related volcanism in the
1097 Neoproterozoic (Cryogenian) Pocatello Formation, SE Idaho: New SHRIMP and CA-ID-TIMS
1098 constraints', *Lithosphere*, vol. 5, no. 1, pp. 128-150. doi:10.1130/L226.1.
1099 Keeman, J, Turner, S, Haines, PW, Belousova, E, Ireland, T, Brouwer, P, Foden, J & Wörner, G 2020,
1100 'New UPb, Hf and O isotope constraints on the provenance of sediments from the Adelaide
1101 Rift Complex – Documenting the key Neoproterozoic to early Cambrian succession',
1102 *Gondwana Research*, vol. 83, pp. 248-278. doi:10.1016/j.gr.2020.02.005.
1103 Keller, CB, Husson, JM, Mitchell, RN, Bottke, WF, Gernon, TM, Boehnke, P, Bell, EA, Swanson-Hysell,
1104 NL & Peters, SE 2019, 'Neoproterozoic glacial origin of the Great Unconformity', *Proc Natl*
1105 *Acad Sci U S A*, vol. 116, no. 4, pp. 1136-1145. doi:10.1073/pnas.1804350116.
1106 Kendall, BS, Creaser, RA, Calver, CR, Raub, TD & Evans, DAD 2009, 'Correlation of Sturtian diamictite
1107 successions in southern Australia and northwestern Tasmania by Re–Os black shale
1108 geochronology and the ambiguity of “Sturtian”-type diamictite–cap carbonate pairs as
1109 chronostratigraphic marker horizons', *Precambrian Research*, vol. 172, no. 3-4, pp. 301-310.
1110 doi:10.1016/j.precamres.2009.05.001.
1111 Kendall, BS, Creaser, RA, Ross, GM & Selby, D 2004, 'Constraints on the timing of Marinoan “Snowball
1112 Earth” glaciation by 187Re–187Os dating of a Neoproterozoic, post-glacial black shale in
1113 Western Canada', *Earth and Planetary Science Letters*, vol. 222, no. 3, pp. 729-740.
1114 doi:10.1016/j.epsl.2004.04.004.
1115 Kendall, BS, Creaser, RA & Selby, D 2006, 'Re-Os geochronology of postglacial black shales in
1116 Australia: Constraints on the timing of “Sturtian” glaciation', *Geology*, vol. 34, no. 9, pp. 729-
1117 732. doi:10.1130/g22775.1.
1118 Kennedy, K, Eyles, N & McArthur, A 2020, 'Syn-rift mass flow generated ‘tectonofacies’ and
1119 ‘tectonosequences’ of the Kingston Peak Formation, Death Valley, California, and their
1120 bearing on supposed Neoproterozoic panglacial climates', *Sedimentology*, vol. 68, no. 1, pp.
1121 352-381. doi:10.1111/sed.12781.
1122 Key, RM, Liyungu, AK, Njamu, FM, Somwe, V, Banda, J, Mosley, PN & Armstrong, RA 2001, 'The
1123 western arm of the Lufilian Arc in NW Zambia and its potential for copper mineralization',
1124 *Journal of African Earth Sciences*, vol. 33, no. 3, pp. 503-528. doi:10.1016/S0899-
1125 5362(01)00098-7.

1126 Knoll, AH, Walter, MR, Narbonne, GM & Christie-Blick, N 2006, 'The Ediacaran Period: a new addition
1127 to the geologic time scale', *Lethaia*, vol. 39, no. 1, pp. 13-30.
1128 doi:10.1080/00241160500409223.

1129 Kochnev, BB, Pokrovskii, BG & Proshenkin, AI 2015, 'The Upper Neoproterozoic glacial complex in
1130 central areas of the Siberian platform', *Doklady Earth Sciences*, vol. 464, no. 2, pp. 1001-
1131 1004. doi:10.1134/s1028334x15100049.

1132 Korsch, RJ, Huston, DL, Henderson, RA, Blewett, RS, Withnall, IW, Fergusson, CL, Collins, WJ, Saygin,
1133 E, Kositcin, N, Meixner, AJ, Chopping, R, Henson, PA, Champion, DC, Hutton, LJ, Wormald, R,
1134 Holzschuh, J & Costelloe, RD 2012, 'Crustal architecture and geodynamics of North
1135 Queensland, Australia: Insights from deep seismic reflection profiling', *Tectonophysics*, vol.
1136 572-573, pp. 76-99. doi:10.1016/j.tecto.2012.02.022.

1137 Krasnobae, AA, Puchkov, VN, Sergeeva, ND & Busharina, SV 2019, 'Nature of zircon clastics in the
1138 Riphean and Vendian sandstones of the Southern Urals', *Georesursy*, vol. 21, no. 1, pp. 15-25.
1139 doi:10.18599/grs.2019.1.15-25.

1140 Kromkhun, K, Foden, JD, Hore, SB & Baines, G 2013, 'Geochronology and Hf isotopes of the bimodal
1141 mafic–felsic high heat producing igneous suite from Mt Painter Province, South Australia',
1142 *Gondwana Research*, vol. 24, no. 3-4, pp. 1067-1079. doi:10.1016/j.gr.2013.01.011.

1143 Kruse, PD, Dunster, JN & Munson, TJ 2013, 'Chapter 28: Georgina Basin', in M Ahmad & TJ Munson
1144 (eds), *Geology and mineral resources of the Northern Territory*, Northern Territory Geological
1145 Survey, Northern Territory.

1146 Lamothe, KG, Hoffman, PF, Greenman, JW & Halverson, GP 2019, 'Stratigraphy and isotope
1147 geochemistry of the pre-Sturtian Ugab Subgroup, Otavi/Swakop Group, northwestern
1148 Namibia', *Precambrian Research*, vol. 332, p. 105387.
1149 doi:10.1016/j.precamres.2019.105387.

1150 Lan, Z, Huyskens, MH, Lu, K, Li, X-H, Zhang, G, Lu, D & Yin, Q-Z 2020, 'Toward refining the onset age
1151 of Sturtian glaciation in South China', *Precambrian Research*, vol. 338.
1152 doi:10.1016/j.precamres.2019.105555.

1153 Lan, Z, Li, X-H, Zhu, M, Zhang, Q & Li, Q-L 2015, 'Revisiting the Liantuo Formation in Yangtze Block,
1154 South China: SIMS U–Pb zircon age constraints and regional and global significance',
1155 *Precambrian Research*, vol. 263, pp. 123-141. doi:10.1016/j.precamres.2015.03.012.

1156 Lan, Z, Li, X, Zhu, M, Chen, Z-Q, Zhang, Q, Li, Q, Lu, D, Liu, Y & Tang, G 2014, 'A rapid and synchronous
1157 initiation of the wide spread Cryogenian glaciations', *Precambrian Research*, vol. 255, pp.
1158 401-411. doi:10.1016/j.precamres.2014.10.015.

1159 Le Heron, DP 2012, 'The Cryogenian record of glaciation and deglaciation in South Australia',
1160 *Sedimentary Geology*, vol. 243-244, pp. 57-69. doi:10.1016/j.sedgeo.2011.09.013.

1161 Le Heron, DP, Busfield, ME, Ali, DO, Al Tofaif, S & Vandyk, TM 2018, 'The Cryogenian record in the
1162 southern Kingston Range, California: The thickest Death Valley succession in the hunt for a
1163 GSSP', *Precambrian Research*, vol. 319, pp. 158-172. doi:10.1016/j.precamres.2017.07.017.

1164 Le Heron, DP, Busfield, ME & Collins, AS 2014, 'Bolla Bollana boulder beds: A Neoproterozoic trough
1165 mouth fan in South Australia?', *Sedimentology*, vol. 61, no. 4, pp. 978-995.
1166 doi:10.1111/sed.12082.

1167 Le Heron, DP, Cox, GM, Trundle, A & Collins, AS 2011, 'Two Cryogenian glacial successions
1168 compared: Aspects of the Sturt and Elatina sediment records of South Australia',
1169 *Precambrian Research*, vol. 186, no. 1, pp. 147-168. doi:10.1016/j.precamres.2011.01.014.

1170 Le Heron, DP, Eyles, N & Busfield, ME 2020, 'The Laurentian Neoproterozoic Glacial Interval:
1171 reappraising the extent and timing of glaciation', *Austrian Journal of Earth Sciences*, vol. 113,
1172 no. 1, pp. 59-70. doi:10.17738/ajes.2020.0004.

1173 Lechte, MA & Wallace, MW 2015, 'Sedimentary and tectonic history of the Holowilena Ironstone, a
1174 Neoproterozoic iron formation in South Australia', *Sedimentary Geology*, vol. 329, pp. 211-
1175 224. doi:10.1016/j.sedgeo.2015.09.014.

1176 Lechte, MA, Wallace, MW, Hood, AvS, Li, W, Jiang, G, Halverson, GP, Asael, D, McColl, SL & Planavsky,
1177 NJ 2019, 'Subglacial meltwater supported aerobic marine habitats during Snowball Earth',
1178 *Proc Natl Acad Sci U S A*, vol. 116, no. 51, pp. 25478-25483.
1179 doi:10.1073/pnas.1909165116.
1180 Lechte, MA, Wallace, MW, Hood, AvS & Planavsky, N 2018, 'Cryogenian iron formations in the
1181 glaciogenic Kingston Peak Formation, California', *Precambrian Research*, vol. 310, pp. 443-
1182 462. doi:10.1016/j.precamres.2018.04.003.
1183 Li, XH, Abd El-Rahman, Y, Abu Anbar, M, Li, J, Ling, XX, Wu, LG & Masoud, AE 2018, 'Old Continental
1184 Crust Underlying Juvenile Oceanic Arc: Evidence From Northern Arabian-Nubian Shield,
1185 Egypt', *Geophysical Research Letters*, vol. 45, no. 7, pp. 3001-3008.
1186 doi:10.1002/2018gl077121.
1187 Link, PK 1977, 'Facies and palaeogeography of Late Precambrian Sturtian glacial sediments, Copley
1188 area, northern Flinders Ranges and in the Sturt Gorge near Adelaide, South Australia',
1189 Department of Geology and Mineralogy, Honours Thesis, Bachelor of Science (Honours),
1190 University of Adelaide, Adelaide, <<https://hdl.handle.net/2440/131122>>.
1191 Link, PK & Christie-Blick, N 2011, 'Neoproterozoic strata of southeastern Idaho and Utah: record of
1192 Cryogenian rifting and glaciation', in E Arnaud, GP Halverson & GA Shields-Zhou (eds), *The
1193 Geological Record of Neoproterozoic Glaciations*, Geological Society, London, pp. 425-436.
1194 Link, PK & Gostin, VA 1981, 'Facies and paleogeography of Sturtian glacial strata (late Precambrian),
1195 South Australia', *American Journal of Science*, vol. 281, no. 4, p. 353.
1196 doi:10.2475/ajs.281.4.353.
1197 Lloyd, JC, Blades, ML, Counts, JW, Collins, AS, Amos, KJ, Wade, BP, Hall, JW, Hore, S, Ball, AL, Shahin,
1198 S & Drabsch, M 2020, 'Neoproterozoic geochronology and provenance of the Adelaide
1199 Superbasin', *Precambrian Research*, vol. 350, p. 105849.
1200 doi:10.1016/j.precamres.2020.105849.
1201 [Preprint] Lloyd, JC, Collins, AS, Blades, ML, Gilbert, SE & Amos, KJ 2022a, 'Early evolution of the
1202 Adelaide Superbasin', *EarthArXiv*. doi:10.31223/X5NH0G.
1203 [Dataset] Lloyd, JC, Collins, AS, Blades, ML, Gilbert, SE & Amos, KJ 2022b, 'LA-ICP-MS detrital zircon
1204 standards results', *figshare*. doi:10.6084/m9.figshare.18131432.
1205 [Preprint] Lloyd, JC, Collins, AS, Blades, ML, Gilbert, SE & Amos, KJ 2022c, 'Late Tonian development
1206 of the Adelaide Superbasin', *EarthArXiv*. doi:10.31223/X5N63H.
1207 [Dataset] Lloyd, JC, Collins, AS, Blades, ML, Gilbert, SE & Amos, KJ 2022d, 'Yudnamutana Subgroup
1208 detrital zircon dataset (Lloyd et al.)', *figshare*. doi:10.6084/m9.figshare.19181144.v1.
1209 Lund, K, Aleinikoff, JN & Evans, KV 2011, 'The Edwardsburg Formation and related rocks,
1210 Windermere Supergroup, central Idaho, USA', in E Arnaud, GP Halverson & GA Shields-Zhou
1211 (eds), *The Geological Record of Neoproterozoic Glaciations*, Geological Society, London, pp.
1212 437-448.
1213 Lund, K, Aleinikoff, JN, Evans, KV, duBray, EA, Dewitt, EH & Unruh, DM 2010, 'SHRIMP U-Pb dating of
1214 recurrent Cryogenian and Late Cambrian–Early Ordovician alkalic magmatism in central
1215 Idaho: Implications for Rodinian rift tectonics', *GSA Bulletin*, vol. 122, no. 3-4, pp. 430-453.
1216 doi:10.1130/B26565.1.
1217 Lund, K, Aleinikoff, JN, Evans, KV & Fanning, CM 2003, 'SHRIMP U-Pb geochronology of
1218 Neoproterozoic Windermere Supergroup, central Idaho: Implications for rifting of western
1219 Laurentia and synchronicity of Sturtian glacial deposits', *GSA Bulletin*, vol. 115, no. 3, pp. 349-
1220 372. doi:10.1130/0016-7606(2003)115<0349:SUPGON>2.0.CO;2.
1221 Macdonald, FA, Schmitz, MD, Crowley, JL, Roots, CF, Jones, DS, Maloof, AC, Strauss, JV, Cohen, PA,
1222 Johnston, DT & Schrag, DP 2010, 'Calibrating the Cryogenian', *Science*, vol. 327, no. 5970,
1223 pp. 1241-1243. doi:10.1126/science.1183325.
1224 Macdonald, FA, Schmitz, MD, Strauss, JV, Halverson, GP, Gibson, TM, Eyster, A, Cox, G, Mamrol, P &
1225 Crowley, JL 2018, 'Cryogenian of Yukon', *Precambrian Research*, vol. 319, pp. 114-143.
1226 doi:10.1016/j.precamres.2017.08.015.

1227 Mackay, WG 2011, 'Structure and sedimentology of the Curdimurka Subgroup, northern Adelaide
1228 Fold Belt, South Australia', Doctoral Thesis, Doctor of Philosophy, University of Tasmania,
1229 Hobart, Tasmania, <<https://eprints.utas.edu.au/12486/>>.

1230 MacLennan, S, Park, Y, Swanson-Hysell, N, Maloof, A, Schoene, B, Gebreslassie, M, Antilla, E, Tesema,
1231 T, Alene, M & Haileab, B 2018, 'The arc of the Snowball: U-Pb dates constrain the Islay
1232 anomaly and the initiation of the Sturtian glaciation', *Geology*, vol. 46, no. 6, pp. 539-542.
1233 doi:10.1130/G40171.1.

1234 Mattinson, JM 2005, 'Zircon U-Pb chemical abrasion ("CA-TIMS") method: Combined annealing and
1235 multi-step partial dissolution analysis for improved precision and accuracy of zircon ages',
1236 *Chemical Geology*, vol. 220, no. 1-2, pp. 47-66. doi:10.1016/j.chemgeo.2005.03.011.

1237 Mawson, D & Sprigg, RC 1950, 'Subdivision of the Adelaide System', *Australian Journal of Science*,
1238 vol. 13, no. 3, pp. 69-72.

1239 McAvaney, SO 2012, 'The Cooyerdoo Granite: Paleo- and Mesoarchean basement of the Gawler
1240 Craton', *MESA Journal*, vol. 65, pp. 31-40.
1241 <https://sarigbasis.pir.sa.gov.au/WebtopEw/ws/samref/sarig1/wci/Record?r=0&m=1&w=catno=2035289>.

1242
1243 McDonough, MR & Parrish, RR 1991, 'Proterozoic gneisses of the Malton Complex, near Valemout,
1244 British Columbia: U-Pb ages and Nd isotopic signatures', *Canadian Journal of Earth Sciences*,
1245 vol. 28, no. 8, pp. 1202-1216. doi:10.1139/e91-108.

1246 Meaney, KJ 2012, 'The geochronology and structural evolution of the Warren Inlier and Springfield
1247 Sequence, Mt. Lofty Ranges: Implications for Proterozoic paleogeographic reconstructions',
1248 School of Earth and Environmental Sciences, Honours Thesis, Bachelor of Science (Honours),
1249 University of Adelaide, Adelaide, South Australia, <<https://hdl.handle.net/2440/95177>>.

1250 Meaney, KJ 2017, 'Proterozoic crustal growth in the southeastern Gawler Craton: the development of
1251 the Barossa Complex, and an assessment of the detrital zircon method', Department of
1252 Geology and Geophysics, Doctoral Thesis, Doctor of Philosophy, University of Adelaide,
1253 Adelaide, South Australia, <<https://hdl.handle.net/2440/114255>>.

1254 Merdith, AS, Williams, SE, Müller, RD & Collins, AS 2017, 'Kinematic constraints on the Rodinia to
1255 Gondwana transition', *Precambrian Research*, vol. 299, pp. 132-150.
1256 doi:10.1016/j.precamres.2017.07.013.

1257 Miller, RM 2013, 'Comparative Stratigraphic and Geochronological Evolution of the Northern Damara
1258 Supergroup in Namibia and the Katanga Supergroup in the Lufilian Arc of Central Africa',
1259 *Geoscience Canada*, vol. 40, no. 2, pp. 118 - 140. doi:10.12789/geocanj.2013.40.007.

1260 Morrissey, LJ, Barovich, KM, Hand, M, Howard, KE & Payne, JL 2019, 'Magmatism and metamorphism
1261 at ca. 1.45 Ga in the northern Gawler Craton: The Australian record of rifting within Nuna
1262 (Columbia)', *Geoscience Frontiers*, vol. 10, no. 1, pp. 175-194.
1263 doi:10.1016/j.gsf.2018.07.006.

1264 Morrissey, LJ, Barovich, KM, Hand, M, Howard, KE, Payne, JL & Reid, AJ 2018, 'The final event in the
1265 long evolution of the Gawler Craton: new constraints on 1450 Ma metamorphism and
1266 magmatism', *MESA Journal*, vol. 88, no. 3, pp. 4-11.
1267 <https://sarigbasis.pir.sa.gov.au/WebtopEw/ws/samref/sarig1/image/DDD/MESAJ088004-011.pdf>.

1268
1269 Morrissey, LJ, Hand, M, Wade, BP & Szpunar, MA 2013, 'Early Mesoproterozoic metamorphism in the
1270 Barossa Complex, South Australia: links with the eastern margin of Proterozoic Australia',
1271 *Australian Journal of Earth Sciences*, vol. 60, no. 8, pp. 769-795.
1272 doi:10.1080/08120099.2013.860623.

1273 Mrofka, D & Kennedy, M 2011, 'The Kingston Peak Formation in the eastern Death Valley region', in E
1274 Arnaud, GP Halverson & GA Shields-Zhou (eds), *The Geological Record of Neoproterozoic
1275 Glaciations*, Geological Society, London, pp. 449-458.

1276 Mundil, R, Ludwig, KR, Metcalfe, I & Renne, PR 2004, 'Age and timing of the Permian mass
1277 extinctions: U/Pb dating of closed-system zircons', *Science*, vol. 305, no. 5691, pp. 1760-
1278 1763. doi:10.1126/science.1101012.

1279 Murrell, B, Link, PK & Gostin, VA 1977, 'Evidence for only one Sturtian Glacial Period in the Copley
1280 map area', *Quarterly Geological Notes*, vol. 64, pp. 16-19.
1281 [https://sarigbasis.pir.sa.gov.au/WebtopEw/ws/samref/sarig1/wci/Record?r=0&m=1&w=catn
1282 o=2041398](https://sarigbasis.pir.sa.gov.au/WebtopEw/ws/samref/sarig1/wci/Record?r=0&m=1&w=catno=2041398).

1283 Nascimento, DB, Ribeiro, A, Trouw, RAJ, Schmitt, RS & Passchier, CW 2016, 'Stratigraphy of the
1284 Neoproterozoic Damara Sequence in northwest Namibia: Slope to basin sub-marine mass-
1285 transport deposits and olistolith fields', *Precambrian Research*, vol. 278, pp. 108-125.
1286 doi:10.1016/j.precamres.2016.03.005.

1287 Nascimento, DB, Schmitt, RS, Ribeiro, A, Trouw, RAJ, Passchier, CW & Basei, MAS 2017, 'Depositional
1288 ages and provenance of the Neoproterozoic Damara Supergroup (northwest Namibia):
1289 Implications for the Angola-Congo and Kalahari cratons connection', *Gondwana Research*,
1290 vol. 52, pp. 153-171. doi:10.1016/j.gr.2017.09.006.

1291 Normington, VJ & Donnellan, NC 2020, *Characterisation of the Neoproterozoic succession of the
1292 northeastern Amadeus Basin, Northern Territory*, Record, no. 2020-010, Northern Territory
1293 Geological Survey, <<https://geoscience.nt.gov.au/gemis/ntgsjspui/handle/1/90622>>.

1294 Norris, A & Danyushevsky, L 2018, 'Towards Estimating the Complete Uncertainty Budget of
1295 Quantified Results Measured by LA-ICP-MS', paper presented at Goldschmidt, Boston.

1296 O'Neill, HSC 2016, 'The Smoothness and Shapes of Chondrite-normalized Rare Earth Element
1297 Patterns in Basalts', *Journal of Petrology*, vol. 57, no. 8, pp. 1463-1508.
1298 doi:10.1093/petrology/egw047.

1299 Och, LM & Shields-Zhou, GA 2012, 'The Neoproterozoic oxygenation event: Environmental
1300 perturbations and biogeochemical cycling', *Earth-Science Reviews*, vol. 110, no. 1, pp. 26-57.
1301 doi:10.1016/j.earscirev.2011.09.004.

1302 Park, Y, Swanson-Hysell, NL, MacLennan, SA, Maloof, AC, Gebreslassie, M, Tremblay, MM, Schoene,
1303 B, Alene, M, Anttila, ESC, Tesema, T & Haileab, B 2019, 'The lead-up to the Sturtian Snowball
1304 Earth: Neoproterozoic chemostratigraphy time-calibrated by the Tambien Group of Ethiopia',
1305 *GSA Bulletin*, vol. 132, no. 5-6, pp. 1119-1149. doi:10.1130/B35178.1.

1306 Pawley, MJ, Dutch, RA & Wise, TW 2020, 'The Relationship Between Crustal Architecture,
1307 Deformation, and Magmatism in the Coompana Province, Australia', *Tectonics*, vol. 39, no. 12.
1308 doi:10.1029/2019tc005593.

1309 Petterson, R, Prave, AR & Wernicke, BP 2011, 'Glaciogenic and related strata of the Neoproterozoic
1310 Kingston Peak Formation in the Panamint Range, Death Valley region, California', in E Arnaud,
1311 GP Halverson & GA Shields-Zhou (eds), *The Geological Record of Neoproterozoic Glaciations*,
1312 Geological Society, London, pp. 459-465.

1313 Plumb, KA 1991, 'New Precambrian time scale', *International Union of Geological Sciences*, vol. 14,
1314 no. 2, pp. 139-140. doi:10.18814/epiugs/1991/v14i2/005.

1315 Plumb, KA & James, HL 1986, 'Subdivision of precambrian time: recommendations and suggestions
1316 by the subcommission on precambrian stratigraphy', *Precambrian Research*, vol. 32, no. 1,
1317 pp. 65-92. doi:10.1016/0301-9268(86)90031-8.

1318 Prave, AR, Condon, DJ, Hoffmann, KH, Tapster, S & Fallick, AE 2016, 'Duration and nature of the end-
1319 Cryogenian (Marinoan) glaciation', *Geology*, vol. 44, no. 8, pp. 631-634.
1320 doi:10.1130/G38089.1.

1321 Preiss, WV 1987, *Adelaide Geosyncline—late Proterozoic stratigraphy, sedimentation, palaeontology
1322 and tectonics*, Bulletin, 53, Geological Survey of South Australia, Adelaide, South Australia.

1323 Preiss, WV 1993, 'Neoproterozoic', in JF Drexel, WV Preiss & AJ Parker (eds), *The geology of South
1324 Australia*, vol. 1 The Precambrian, Geological Survey of South Australia, South Australia, pp.
1325 171-204.

- 1326 Preiss, WV 2000, 'The Adelaide Geosyncline of South Australia and its significance in Neoproterozoic
1327 continental reconstruction', *Precambrian Research*, vol. 100, no. 1-3, pp. 21-63.
1328 doi:10.1016/S0301-9268(99)00068-6.
- 1329 Preiss, WV 2006, 'Old Boolcoomata Conglomerate Member of the Benda Siltstone', *MESA Journal*,
1330 vol. 41, pp. 15-23.
1331 [https://sarigbasis.pir.sa.gov.au/WebtopEw/ws/samref/sarig1/wci/Record?r=0&m=1&w=catn
1332 o=2025262](https://sarigbasis.pir.sa.gov.au/WebtopEw/ws/samref/sarig1/wci/Record?r=0&m=1&w=catno=2025262).
- 1333 Preiss, WV, Alexander, EM, Cowley, WM & Schwarz, MP 2002, 'Towards defining South Australia's
1334 geological provinces and sedimentary basins', *MESA Journal*, vol. 27, pp. 39-52.
1335 [https://sarigbasis.pir.sa.gov.au/WebtopEw/ws/samref/sarig1/wci/Record?r=0&m=1&w=catn
1336 o=2022981](https://sarigbasis.pir.sa.gov.au/WebtopEw/ws/samref/sarig1/wci/Record?r=0&m=1&w=catno=2022981).
- 1337 Preiss, WV, Dyson, IA, Reid, PW & Cowley, WM 1998, 'Revision of lithostratigraphic classification of
1338 the Umberatana Group', *MESA Journal*, vol. 9, pp. 36-42.
1339 [https://sarigbasis.pir.sa.gov.au/WebtopEw/ws/samref/sarig1/wcir/Record?r=0&m=1&w=cat
1340 no=2025009](https://sarigbasis.pir.sa.gov.au/WebtopEw/ws/samref/sarig1/wcir/Record?r=0&m=1&w=catno=2025009).
- 1341 Preiss, WV, Gostin, VA, McKirdy, DM, Ashley, PM, Williams, GE & Schmidt, PW 2011, 'The glacial
1342 succession of Sturtian age in South Australia: The Yudnamutana Subgroup', in E Arnaud, GP
1343 Halverson & GA Shields-Zhou (eds), *The Geological Record of Neoproterozoic Glaciations*,
1344 Geological Society, London, pp. 701-712.
- 1345 Preiss, WV, Walter, MR, Coats, RP & Wells, AT 1978, 'Lithological correlations of Adelaidean
1346 glaciogenic rocks in parts of the Amadeus, Ngalia, and Georgina Basins', *AGSO Journal of
1347 Australian Geology and Geophysics*, vol. 3, pp. 43-53.
1348 <http://pid.geoscience.gov.au/dataset/ga/80944>.
- 1349 Reid, A, Tiddy, C, Jagodzinski, E, Crowley, J, Conor, C, Brotodewo, A & Wade, C 2021, *Precise zircon U-
1350 Pb geochronology of Hiltaba Suite granites, Point Riley, Yorke Peninsula*, Report Book, no.
1351 2021/00001, Geological Survey of South Australia, DfEa Mining, South Australia.
- 1352 Reid, AJ, Halpin, JA & Dutch, RA 2019, 'Timing and style of high-temperature metamorphism across
1353 the Western Gawler Craton during the Paleo- to Mesoproterozoic', *Australian Journal of Earth
1354 Sciences*, vol. 66, no. 8, pp. 1085-1111. doi:10.1080/08120099.2019.1602565.
- 1355 Reid, AJ & Hand, M 2012, 'Mesoarchean to Mesoproterozoic evolution of the southern Gawler Craton,
1356 South Australia', *Episodes*, vol. 35, no. 1, pp. 216-225.
1357 doi:10.18814/epiiugs/2012/v35i1/021.
- 1358 Reid, AJ, Hand, M, Jagodzinski, EA, Kelsey, DE & Pearson, NJ 2008, 'Paleoproterozoic orogenesis in
1359 the southeastern Gawler Craton, South Australia', *Australian Journal of Earth Sciences*, vol.
1360 55, no. 4, pp. 449-471. doi:10.1080/08120090801888594.
- 1361 Reid, AJ, Jagodzinski, EA, Armit, RJ, Dutch, RA, Kirkland, CL, Betts, PG & Schaefer, BF 2014a, 'U-Pb
1362 and Hf isotopic evidence for Neoproterozoic and Paleoproterozoic basement in the buried
1363 northern Gawler Craton, South Australia', *Precambrian Research*, vol. 250, pp. 127-142.
1364 doi:10.1016/j.precamres.2014.05.019.
- 1365 Reid, AJ, Jagodzinski, EA, Fraser, GL & Pawley, MJ 2014b, 'SHRIMP U-Pb zircon age constraints on
1366 the tectonics of the Neoproterozoic to early Paleoproterozoic transition within the Mulgathing
1367 Complex, Gawler Craton, South Australia', *Precambrian Research*, vol. 250, pp. 27-49.
1368 doi:10.1016/j.precamres.2014.05.013.
- 1369 Reid, AJ, Jagodzinski, EA, Wade, CE, Payne, JL & Jourdan, F 2017, 'Recognition of c. 1780Ma
1370 magmatism and metamorphism in the buried northeastern Gawler Craton: Correlations with
1371 events of the Aileron Province', *Precambrian Research*, vol. 302, pp. 198-220.
1372 doi:10.1016/j.precamres.2017.09.010.
- 1373 Reid, AJ & Payne, JL 2017, 'Magmatic zircon Lu-Hf isotopic record of juvenile addition and crustal
1374 reworking in the Gawler Craton, Australia', *Lithos*, vol. 292-293, pp. 294-306.
1375 doi:10.1016/j.lithos.2017.08.010.

1376 Rooney, AD, Chew, DM & Selby, D 2011, 'Re–Os geochronology of the Neoproterozoic–Cambrian
1377 Dalradian Supergroup of Scotland and Ireland: Implications for Neoproterozoic stratigraphy,
1378 glaciations and Re–Os systematics', *Precambrian Research*, vol. 185, no. 3-4, pp. 202-214.
1379 doi:10.1016/j.precamres.2011.01.009.

1380 Rooney, AD, Macdonald, FA, Strauss, JV, Dudas, FÖ, Hallmann, C & Selby, D 2014, 'Re-Os
1381 geochronology and coupled Os-Sr isotope constraints on the Sturtian snowball Earth',
1382 *Proceedings of the National Academy of Sciences of the United States of America*, vol. 111, no.
1383 1, pp. 51-56. doi:10.1073/pnas.1317266110.

1384 Rooney, AD, Strauss, JV, Brandon, AD & Macdonald, FA 2015, 'A Cryogenian chronology: Two long-
1385 lasting synchronous Neoproterozoic glaciations', *Geology*, vol. 43, no. 5, pp. 459-462.
1386 doi:10.1130/G36511.1.

1387 Rooney, AD, Yang, C, Condon, DJ, Zhu, M & Macdonald, FA 2020, 'U-Pb and Re-Os geochronology
1388 tracks stratigraphic condensation in the Sturtian snowball Earth aftermath', *Geology*.
1389 doi:10.1130/G47246.1.

1390 Rose, CV, Maloof, AC, Schoene, B, Ewing, RC, Linnemann, U, Hofmann, M & Cottle, JM 2013, 'PAUL F.
1391 HOFFMAN SERIES The End-Cryogenian Glaciation of South Australia', *Geoscience Canada*,
1392 vol. 40, no. 4, pp. 256-293. doi:10.12789/geocanj.2013.40.019.

1393 Ross, GM & Villeneuve, J 1997, *U-Pb geochronology of stranger stones in Neoproterozoic diamictites,*
1394 *Canadian Cordillera: implications for provenance and ages of deposition*, Report, Geological
1395 Survey of Canada, NR Canada.

1396 Rubatto, D 2002, 'Zircon trace element geochemistry: partitioning with garnet and the link between
1397 U–Pb ages and metamorphism', *Chemical Geology*, vol. 184, no. 1, pp. 123-138.
1398 doi:10.1016/S0009-2541(01)00355-2.

1399 Rud`ko, S, Kuznetsov, N, Shatsillo, A, Rud`ko, D, Malyshev, S, Dubenskiy, A, Sheshukov, V, Kanygina,
1400 N & Romanyuk, T 2020, 'Sturtian glaciation in Siberia: Evidence of glacial origin and U-Pb
1401 dating of the diamictites of the Chivida Formation in the north of the Yenisei Ridge',
1402 *Precambrian Research*, vol. 345. doi:10.1016/j.precamres.2020.105778.

1403 Schmitz, MD 2012, 'Radiometric ages used in GTS2012', in FM Gradstein, JG Ogg, MD Schmitz & GM
1404 Ogg (eds), *The Geologic Time Scale*, pp. 1045-1082.

1405 Segnit, RW 1939, *The Precambrian-Cambrian succession - The general and economic geology of*
1406 *these systems, in portions of South Australia*, Bulletin, 18, Department of Mines, Adelaide,
1407 South Australia.

1408 Shannon, RD 1976, 'Revised effective ionic radii and systematic studies of interatomic distances in
1409 halides and chalcogenides', *Acta Crystallographica Section A*, vol. 32, no. 5, pp. 751-767.
1410 doi:10.1107/S0567739476001551.

1411 Shields-Zhou, GA, Porter, SM & Halverson, GP 2016, 'A New Rock-Based Definition for the Cryogenian
1412 Period (Circa 720-635 Ma)', *Episodes*, vol. 39, no. 1.
1413 doi:10.18814/epiiugs/2016/v39i1/89231.

1414 Shields, GA, Halverson, GP & Porter, SM 2018, 'Descent into the Cryogenian', *Precambrian Research*,
1415 vol. 319, pp. 1-5. doi:10.1016/j.precamres.2018.08.015.

1416 Shields, GA, Strachan, RA, Porter, SM, Halverson, GP, Macdonald, FA, Plumb, KA, de Alvarenga, CJ,
1417 Banerjee, DM, Bekker, A, Bleeker, W, Brasier, A, Chakraborty, PP, Collins, AS, Condie, K, Das,
1418 K, Evans, DAD, Ernst, R, Fallick, AE, Frimmel, H, Fuck, R, Hoffman, PF, Kamber, BS, Kuznetsov,
1419 AB, Mitchell, RN, Poiré, DG, Poulton, SW, Riding, R, Sharma, M, Storey, C, Stueeken, E,
1420 Tostevin, R, Turner, E, Xiao, S, Zhang, S, Zhou, Y & Zhu, M 2022, 'A template for an improved
1421 rock-based subdivision of the pre-Cryogenian timescale', *Journal of the Geological Society*,
1422 vol. 179, no. 1. doi:10.1144/jgs2020-222.

1423 Sláma, J & Košler, J 2012, 'Effects of sampling and mineral separation on accuracy of detrital zircon
1424 studies', *Geochemistry Geophysics Geosystems*, vol. 13, no. 5. doi:10.1029/2012gc004106.

1425 Sláma, J, Košler, J, Condon, DJ, Crowley, JL, Gerdes, A, Hanchar, JM, Horstwood, MSA, Morris, GA,
1426 Nasdala, L, Norberg, N, Schaltegger, U, Schoene, B, Tubrett, MN & Whitehouse, MJ 2008,
1427 'Plešovice zircon — A new natural reference material for U–Pb and Hf isotopic microanalysis',
1428 *Chemical Geology*, vol. 249, no. 1, pp. 1-35. doi:10.1016/j.chemgeo.2007.11.005.
1429 Smithies, RH, Howard, HM, Evins, PM, Kirkland, CL, Bodorkos, S & Wingate, MTD 2008, *The west*
1430 *Musgrave Complex - new geological insights from recent mapping, geochronology, and*
1431 *geochemical studies*, Record, no. 2008/19, Geological Survey of Western Australia,
1432 <[http://dmpbookshop.eruditetechnologies.com.au/product/the-west-musgrave-complex-](http://dmpbookshop.eruditetechnologies.com.au/product/the-west-musgrave-complex-new-geological-insights-from-recent-mapping-geochronology-and-geochemical-studies.do)
1433 [new-geological-insights-from-recent-mapping-geochronology-and-geochemical-](http://dmpbookshop.eruditetechnologies.com.au/product/the-west-musgrave-complex-new-geological-insights-from-recent-mapping-geochronology-and-geochemical-studies.do)
1434 [studies.do](http://dmpbookshop.eruditetechnologies.com.au/product/the-west-musgrave-complex-new-geological-insights-from-recent-mapping-geochronology-and-geochemical-studies.do)>.
1435 Smithies, RH, Howard, HM, Evins, PM, Kirkland, CL, Kelsey, DE, Hand, M, Wingate, MTD, Collins, AS &
1436 Belousova, EA 2011, 'High-Temperature Granite Magmatism, Crust–Mantle Interaction and
1437 the Mesoproterozoic Intracontinental Evolution of the Musgrave Province, Central Australia',
1438 *Journal of Petrology*, vol. 52, no. 5, pp. 931-958. doi:10.1093/petrology/egr010.
1439 Smits, RG, Collins, WJ, Hand, M, Dutch, R & Payne, J 2014, 'A Proterozoic Wilson cycle identified by
1440 Hf isotopes in central Australia: Implications for the assembly of Proterozoic Australia and
1441 Rodinia', *Geology*, vol. 42, no. 3, pp. 231-234. doi:10.1130/g35112.1.
1442 Song, G, Wang, X, Shi, X & Jiang, G 2017, 'New U-Pb age constraints on the upper Banxi Group and
1443 synchrony of the Sturtian glaciation in South China', *Geoscience Frontiers*, vol. 8, no. 5, pp.
1444 1161-1173. doi:10.1016/j.gsf.2016.11.012.
1445 Sprigg, RC 1952, 'Sedimentation in the Adelaide Geosyncline and the formation of the continental
1446 terrace', in MF Glaessner & RC Sprigg (eds), *Sir Douglas Mawson Anniversary Volume*, The
1447 University of Adelaide, South Australia, pp. 153-159.
1448 Stevens, BPJ, Page, RW & Crooks, A 2008, 'Geochronology of Willyama Supergroup metavolcanics,
1449 metasediments and contemporaneous intrusions, Broken Hill, Australia', *Australian Journal*
1450 *of Earth Sciences*, vol. 55, no. 3, pp. 301-330. doi:10.1080/08120090701769456.
1451 Strauss, JV, Rooney, AD, Macdonald, FA, Brandon, AD & Knoll, AH 2014, '740 Ma vase-shaped
1452 microfossils from Yukon, Canada: Implications for Neoproterozoic chronology and
1453 biostratigraphy', *Geology*, vol. 42, no. 8, pp. 659-662. doi:10.1130/G35736.1.
1454 Swain, G, Woodhouse, A, Hand, M, Barovich, K, Schwarz, M & Fanning, CM 2005, 'Provenance and
1455 tectonic development of the late Archaean Gawler Craton, Australia; U–Pb zircon,
1456 geochemical and Sm–Nd isotopic implications', *Precambrian Research*, vol. 141, no. 3, pp.
1457 106-136. doi:10.1016/j.precamres.2005.08.004.
1458 Sweet, IP & Preiss, WV 1966, 'The Geology of the Depot Creek Area, Flinders Ranges, South
1459 Australia', Geology & Geophysics, Honours Thesis, Bachelor of Science (Honours), University
1460 of Adelaide, Adelaide, South Australia, <<https://hdl.handle.net/2440/8536>>.
1461 Thomson, BP, Coats, RP, Mirams, RC, Forbes, BG, Dalgarno, CR & Johnson, JE 1964, 'Precambrian
1462 Rock Groups in the Adelaide Geosyncline: A new subdivision', *Quarterly Geological Notes*, vol.
1463 9, pp. 1-20.
1464 Tostevin, R & Mills, BJW 2020, 'Reconciling proxy records and models of Earth's oxygenation during
1465 the Neoproterozoic and Palaeozoic', *Interface Focus*, vol. 10, no. 4, p. 20190137.
1466 doi:10.1098/rsfs.2019.0137.
1467 van der Wolff, EJ 2020, 'Detrital Provenance and Geochronology of the Burra, Umberatana and
1468 Wilpena Groups in the Mount Lofty Ranges', Department of Earth Sciences, Honours Thesis,
1469 Bachelor of Science (Honours), University of Adelaide, Adelaide, South Australia.
1470 Verdel, C, Campbell, MJ & Allen, CM 2021, 'Detrital zircon petrochronology of central Australia, and
1471 implications for the secular record of zircon trace element composition', *Geosphere*.
1472 doi:10.1130/ges02300.1.
1473 Vermeesch, P 2018, 'IsoplotR: a free and open toolbox for geochronology', *Geoscience Frontiers*, vol.
1474 9, no. 5. doi:10.1016/j.gsf.2018.04.001.

- 1475 Vermeesch, P, Resentini, A & Garzanti, E 2016, 'An R package for statistical provenance analysis',
1476 *Sedimentary Geology*, vol. 336, pp. 14-25. doi:10.1016/j.sedgeo.2016.01.009.
- 1477 Virgo, GM, Collins, AS, Amos, KJ, Farkaš, J, Blades, ML & Subarkah, D 2021, 'Descending into the
1478 "snowball": High resolution sedimentological and geochemical analysis across the Tonian to
1479 Cryogenian boundary in South Australia', *Precambrian Research*, vol. 367.
1480 doi:10.1016/j.precamres.2021.106449.
- 1481 Wade, BP, Kelsey, DE, Hand, M & Barovich, KM 2008, 'The Musgrave Province: Stitching north, west
1482 and south Australia', *Precambrian Research*, vol. 166, no. 1, pp. 370-386.
1483 doi:10.1016/j.precamres.2007.05.007.
- 1484 Wade, CE 2011, 'Definition of the Mesoproterozoic Ninnerie Supersuite, Curnamona Province, South
1485 Australia', *MESA Journal*, vol. 62, pp. 25-42.
- 1486 Wallace, MW, Hood, Av, Shuster, A, Greig, A, Planavsky, NJ & Reed, CP 2017, 'Oxygenation history of
1487 the Neoproterozoic to early Phanerozoic and the rise of land plants', *Earth and Planetary
1488 Science Letters*, vol. 466, pp. 12-19. doi:10.1016/j.epsl.2017.02.046.
- 1489 Wallace, MW, Hood, AvS, Woon, EMS, Giddings, JA & Fromhold, TA 2015, 'The Cryogenian
1490 Balcanoona reef complexes of the Northern Flinders Ranges: Implications for Neoproterozoic
1491 ocean chemistry', *Palaeogeography, Palaeoclimatology, Palaeoecology*, vol. 417, pp. 320-
1492 336. doi:10.1016/j.palaeo.2014.09.028.
- 1493 Wang, D, Zhu, X-K, Zhao, N, Yan, B, Li, X-H, Shi, F & Zhang, F 2019, 'Timing of the termination of
1494 Sturtian glaciation: SIMS U-Pb zircon dating from South China', *Journal of Asian Earth
1495 Sciences*, vol. 177, pp. 287-294. doi:10.1016/j.jseaes.2019.03.015.
- 1496 Wiedenbeck, M, Allé, P, Corfu, F, Griffin, WL, Meier, M, Oberli, F, Quadt, AV, Roddick, JC & Spiegel, W
1497 1995, 'Three Natural Zircon Standards for U-Th-Pb, Lu-Hf, Trace Element and REE Analyses',
1498 *Geostandards Newsletter*, vol. 19, no. 1, pp. 1-23. doi:10.1111/j.1751-
1499 908X.1995.tb00147.x.
- 1500 Wiedenbeck, M, Hanchar, JM, Peck, WH, Sylvester, P, Valley, J, Whitehouse, M, Kronz, A, Morishita, Y,
1501 Nasdala, L, Fiebig, J, Franchi, I, Girard, JP, Greenwood, RC, Hinton, R, Kita, N, Mason, PRD,
1502 Norman, M, Ogasawara, M, Piccoli, PM, Rhede, D, Satoh, H, Schulz-Dobrick, B, Skår, O,
1503 Spicuzza, MJ, Terada, K, Tindle, A, Togashi, S, Vennemann, T, Xie, Q & Zheng, YF 2004,
1504 'Further Characterisation of the 91500 Zircon Crystal', *Geostandards and Geoanalytical
1505 Research*, vol. 28, no. 1, pp. 9-39. doi:10.1111/j.1751-908X.2004.tb01041.x.
- 1506 Williams, GE & Gostin, VA 2019, 'Late Cryogenian glaciation in South Australia: Fluctuating ice margin
1507 and no extreme or rapid post-glacial sea-level rise', *Geoscience Frontiers*.
1508 doi:10.1016/j.gsf.2019.02.002.
- 1509 Wu, L, Guan, S, Ren, R, Zhang, C & Feng, X 2019, 'Neoproterozoic glaciations and rift evolution in the
1510 northwest Tarim Craton, China: new constraints from geochronological, geochemical, and
1511 geophysical data', *International Geology Review*, pp. 1-20.
1512 doi:10.1080/00206814.2019.1700399.
- 1513 Wysoczanski, RJ & Allibone, AH 2004, 'Age, Correlation, and Provenance of the Neoproterozoic
1514 Skelton Group, Antarctica: Grenville Age Detritus on the Margin of East Antarctica', *Journal of
1515 Geology*, vol. 112, no. 4, pp. 401-416. doi:10.1086/421071.
- 1516 Xiao, W, Cao, J, Luo, B, He, Y, Zhou, G, Zuo, Z, Xiao, D & Hu, K 2020, 'Marinoan glacial aftermath in
1517 South China: Paleo-environmental evolution and organic carbon accumulation in the
1518 Doushantuo shales', *Chemical Geology*, vol. 555, p. 119838.
1519 doi:10.1016/j.chemgeo.2020.119838.
- 1520 Xu, B, Xiao, S, Zou, H, Chen, Y, Li, Z-X, Song, B, Liu, D, Zhou, C & Yuan, X 2009, 'SHRIMP zircon U-Pb
1521 age constraints on Neoproterozoic Quruqtagh diamictites in NW China', *Precambrian
1522 Research*, vol. 168, no. 3, pp. 247-258. doi:10.1016/j.precamres.2008.10.008.

- 1523 Young, GM & Gostin, VA 1989a, 'Depositional environment and regional stratigraphic significance of
1524 the Serle Conglomerate: A Late Proterozoic submarine fan complex, South Australia',
1525 *Palaeogeography, Palaeoclimatology, Palaeoecology*, vol. 71, no. 3, pp. 237-252.
1526 doi:10.1016/0031-0182(89)90052-7.
- 1527 Young, GM & Gostin, VA 1989b, 'An exceptionally thick upper Proterozoic (Sturtian) glacial succession
1528 in the Mount Painter area, South Australia', *Geological Society of America Bulletin*, vol. 101,
1529 no. 6, pp. 834-845. doi:10.1130/0016-7606(1989)101<0834:Aetups>2.3.Co;2.
- 1530 Young, GM & Gostin, VA 1991, 'Late Proterozoic (Sturtian) succession of the North Flinders Basin,
1531 South Australia; An example of temperate glaciation in an active rift setting', in JB Anderson
1532 & GM Ashley (eds), *Glacial marine sedimentation; Paleoclimatic significance*, vol. 261,
1533 Geological Society of America, p. 0.
- 1534 Zaitseva, TS, Kuznetsov, AB, Gorozhanin, VM, Gorokhov, IM, Ivanovskaya, TA & Konstantinova, GV
1535 2019, 'The Lower Boundary of the Vendian in the Southern Urals as Evidenced by the Rb–Sr
1536 Age of Glauconites of the Bakeevo Formation', *Stratigraphy and Geological Correlation*, vol.
1537 27, no. 5, pp. 573-587. doi:10.1134/s0869593819050083.
- 1538 Zhang, Q-R, Chu, X-L & Feng, L-J 2011, 'Neoproterozoic glacial records in the Yangtze Region, China',
1539 in E Arnaud, GP Halverson & GA Shields-Zhou (eds), *The Geological Record of Neoproterozoic*
1540 *Glaciations*, Geological Society, London, pp. 357-366.
- 1541 Zhang, Q-R, Li, X-H, Feng, L-J, Huang, J & Song, B 2008, 'A New Age Constraint on the Onset of the
1542 Neoproterozoic Glaciations in the Yangtze Platform, South China', *The Journal of Geology*, vol.
1543 116, no. 4, pp. 423-429. doi:10.1086/589312.
- 1544 Zhang, S, Jiang, G, Zhang, J, Song, B, Kennedy, MJ & Christie-Blick, N 2005, 'U-Pb sensitive high-
1545 resolution ion microprobe ages from the Doushantuo Formation in south China: Constraints
1546 on late Neoproterozoic glaciations', *Geology*, vol. 33, no. 6. doi:10.1130/g21418.1.
- 1547 Zhou, C-M, Huyskens, MH, Xiao, S & Yin, Q-Z 2020, 'Refining the termination age of the Cryogenian
1548 Sturtian glaciation in South China', *Palaeoworld*, vol. 29, no. 3, pp. 462-468.
1549 doi:10.1016/j.palwor.2020.04.002.
- 1550 Zhou, C, Huyskens, MH, Lang, X, Xiao, S & Yin, Q-Z 2019, 'Calibrating the terminations of Cryogenian
1551 global glaciations', *Geology*, vol. 47, no. 3, pp. 251-254. doi:10.1130/g45719.1.
- 1552 Zhou, C, Tucker, R, Xiao, S, Peng, Z, Yuan, X & Chen, Z 2004, 'New constraints on the ages of
1553 Neoproterozoic glaciations in south China', *Geology*, vol. 32, no. 5, pp. 437-440.
1554 doi:10.1130/G20286.1.
- 1555 Zhu, M & Wang, H 2011, 'Neoproterozoic glaciogenic diamictites of the Tarim Block, NW China', in E
1556 Arnaud, GP Halverson & GA Shields-Zhou (eds), *The Geological Record of Neoproterozoic*
1557 *Glaciations*, Geological Society, London, pp. 367-378.

1558

1559

APPENDIX 1 - DEFINITION CARD

NAME OF UNIT ¹ : Sturt Formation	STATE(S) ¹ : South Australia
STATUS OF UNIT : Redefinition	RANK : Formation
PROPOSER : Jarred C Lloyd, Wolfgang V Preiss, Georgina M Virgo	DATE : 2022-02-
RESERVED IN STRATIGRAPHIC UNITS DATABASE : YES	
PROPOSED PUBLICATION : Lloyd, JC, Preiss, WV, Collins, AS, Virgo, GM, Blades, ML & Amos, KJ [in prep], 'Detrital zircon record of the Sturtian glaciation: Adelaide Superbasin', to be submitted to <i>Geological Magazine</i> , (EarthArXiv preprint, this publication)	

1560

DERIVATION OF NAME ¹ : Sturt River/Warriparri, South Australia
<p>SYNONYMY, UNIT NAME HISTORY (if any) ¹:</p> <p>Sturt Tillite, Appila Tillite, Pualco Tillite, Merinjina Tillite, Bolla Bollana Tillite, Calthorinna Tillite, Hansborough Tillite (abandoned)</p> <p>Originally named the Sturtian Tillite (Howchin, 1920)</p>
CONSTITUENT UNITS ³ : Braemar ironstone facies (informal)
PARENT UNIT : Yudnamutana Subgroup
<p>TYPE LOCALITY (including Lat. & Long.) ²:</p> <p>CRS for all coordinates is EPSG:7844 (GDA2020); estimations use historical data and modern remote sensing imagery and GIS data to provide locations that are as accurate as possible.</p> <p>Primary type: SW of Mount Harris, through MacDonnell Creek – base: 139.357, -30.095, top: 139.34021, -30.07363 (GDA2020)</p> <p>Reference sections:</p> <ul style="list-style-type: none"> • Sturt Gorge Recreation Park – base: 138.59633, -35.03398, top: 138.57289, -35.03947 (GDA2020, composite section, estimated from georeferenced map of Link 1977 and current boundaries shown on 100K surface) • Appila Gorge – base: 138.48247, -33.00312, top: 138.48458, -33.00341 (GDA2020, estimated based on section map from Segnit 1939) • Pualco Hill – base: 139.64033, -32.97827, top: 139.60483, -32.95732 (GDA2020, composite section, estimated location from map and detail in QGN 60) • NW of Copley – base: 138.38933, -30.56145, top: 138.39032, -30.5592 (GDA2020) • Termination Hill – base: 138.01746, -30.21562, top: 138.01387, -30.21756 (GDA2020) • Yankaninna Station – base: 138.94295, -30.28636, top: 138.9431, -30.28593, (GDA2020, northern section); base: 138.99635, -30.36184, top: 138.9976, -30.36354 (GDA2020, southern section) • Davenport and Denison Ranges – base: 135.94206, -28.68947, top: 135.93648, -28.70065 (GDA2020, estimated from Ambrose et al. 1981)

- Tillite Gorge, Arkaroola – base: 139.43277, -30.33123, top: 139.40406, -30.34282 (GDA2020)

CONFIDENTIAL TYPE LOCALITY?: No

DESCRIPTION AT TYPE LOCALITY ²:

The Sturt Formation comprises characteristic (boulder) diamictites showing evidence for glaciogenic origin, and numerous subsidiary lithologies including poorly sorted sandstones/conglomerates through to finely laminated shales containing a wide variety of limestones and dropstones.

LITHOLOGY ²:

The lithology of the Sturt Formation at its type section defined here is further detailed in Belperio (1973) and Young & Gostin (1989). It is subdivided into four generalised lithologies:

Unit 1: Very poorly sorted conglomerates with sandy matrix to true diamictites with muddy, silty and even very fine sandy matrix. Clasts ranging in size up to boulder (largest observed: 1 m); minor interbeds of laminated siltstone. A higher concentration of larger clast sizes is present in the lower sections.

Unit 2: Interbedded, well laminated shales and sandy micaceous siltstones. Minor pebbly lenses and silty arenites, crossbedding present, and ripple marked.

Unit 3: Crudely stratified diamictite (lithic wacke, muddy to silty matrix) with clasts ranging up to boulder size (max. observed: 90 cm). Minor interbeds of calcareous shale, and thick interbeds of massive diamictite.

Unit 4: Similar to unit 3, however has a higher mud content in matrix and is mostly massive diamictite. Greater number and size of clasts, ranging up to 1.25 m (observed).

THICKNESS ²: ~1,470 m at primary type section

FOSSILS: N/A

DIASTEMS OR HIATUSES (if relevant): N/A

RELATIONSHIPS & BOUNDARY CRITERIA ²:

Most commonly overlies Burra Group, less commonly Callanna Group or pre-Neoproterozoic basement. Conformably overlain by Holowilena Ironstone, Benda Siltstone, Wilyerpa Formation, and Lyndhurst Formation. Disconformably overlain by Tapley Hill Formation where Wilyerpa Formation is absent, e.g. Sturt Gorge.

DISTINGUISHING OR IDENTIFYING FEATURES ¹:

Poorly sorted, massive diamictite with clasts ranging up to extremely large boulders. These significantly differ lithologically from the over- and underlying strata. Evidence for glaciogenic origin (dropstones in laminated rocks [limestones that warp and/or puncture the underlying laminae]; glacial striae and scouring of underlying rock; presence of polished, faceted, striated and grooved clasts) can often be found in outcrop; one glaciated pavement near Merinjina Well.

AGE & EVIDENCE ²:

Minimum: 663 ± 0.76 Ma (Tuff near base of overlying Wilyerpa Formation, Cox et al. 2018)

Detrital zircon max depositional age (upper Sturt Formation):

- 667 ± 6 Ma (Pichi Richi Pass, Keeman et al. 2020; data reinterpreted in Lloyd et al. 2020)
- 666 ± 25 Ma (Copley, Lloyd et al. 2022a [pre-print])
- 673 ± 19 Ma (Willouran Ranges, Lloyd et al. 2020)

Maximum age: constrained to younger than 731 ± 34 Ma by detrital zircon in the underlying Gilbert Range Quartzite (Keeman et al. 2020; data reinterpreted in Lloyd et al. 2020) and corroborated by detrital zircon in the Mitcham Quartzite, 734 ± 42 Ma (Lloyd et al. 2022b [pre-print]).

CORRELATION WITH OTHER UNITS ²:

Stratigraphic relative of the Chambers Bluff Tillite (Officer Basin), Areyonga Formation (Amadeus Basin), Naburula Formation (Ngalia Basin), Yardida Tillite (Georgina Basin), and lower units of the Yancowinna Subgroup (NSW). Potential correlatives in Tasmania are the Julius River Member, Red Rock Member, Cotcase Creek Formation, and middle Port Sorrel Formation.

REGIONAL ASPECTS/GENERAL GEOLOGICAL DESCRIPTION:

General lithologic sequence common throughout the basin in complete, or near complete successions of the Sturt Formation is:

- poorly sorted, gravel to boulder conglomerate (diamictite in some areas) with generally sandy matrix; scoured bases are common in areas where the Fitton Formation is not present
- Interbedded fine laminated siltstones and shales to cross-bedded sandstones with few limestones/dropstones
- boulder diamictite (both massive and stratified)

Regionally, the size, composition, and percentage of clasts in the diamictite lithologies varies. Mega-clasts, ranging up to 1.25 km have been described in the MacDonald corridor north of Olary (Conor & Preiss, 2019).

Arkosic, poorly sorted immature sandstones, and cross-bedded sandstones are predominant in some areas. Iron-rich sections are present in the Sturt Formation underlying the Benda Siltstone and Holowilena Ironstone in the Nackara Arc/South Flinders Ranges.

EXTENT:

Deposited across the entire Adelaide Rift Complex within the Adelaide Superbasin; local areas of non-deposition or subsequent erosion. Deposition on the Stuart Shelf appears to be limited to the eastern most areas and deposition on the Coomalarnie Platform is not known.

GEOMORPHIC EXPRESSION:

THICKNESS VARIATIONS: Thickness varies greatly because of palaeotopography, palaeotectonic activity, and erosion.

Minimum: 9 m, ~2.5 km to the NW of Tower Hill (Mount Lyndhurst station)

Maximum: 3,300 m at Pualco Hill.

STRUCTURE AND METAMORPHISM:

ALTERATION AND MINERALISATION: Iron rich facies present in the Nackara Arc; Talc, Au,

Cu, Pb mineralised zones have also been found.

GEOPHYSICAL EXPRESSION:

Iron rich facies show strong anomaly on TMI where the original hematite (as in the Holowilena Ironstone) has been metamorphosed to magnetite (as in Braemar ironstone facies of the Benda Siltstone and the Pualco Range outcrops of the Sturt Formation.

Surface exposure can be readily identified using false colour remote sensing imagery, for LANDSAT 8 specifically using channels 7-5-2 and 5-6-7 for R-G-B.

GEOCHEMISTRY:

GENESIS/DEPOSITIONAL ENVIRONMENT:

Deposited under general glaciogenic conditions: dropstones, lonestones, glacial striae, mega-clasts. Exact environment is dependent on location but encompasses the full range of sub-glacial to pro-glacial terrestrial and glacio-marine sedimentary environments. Mostly massive but contains lithologies showing planar stratification, cross stratification, reverse graded bedding, scour structures, and ripple laminations.

The cast of a glaciated pavement is preserved near Merinjina Well where the Sturt Formation disconformably overlies the Wooltana Volcanics.

COMMENTS:

The “Tillite” portion of the name has been dropped in favour for “Formation” in contrast to the reasoning outlined in Coats & Preiss (1987). This change is done to better reflect the diversity in lithologies present throughout the Sturt Formation. The most prominent of these are the diamictites, many of which are shown to be true tillites, however the formation varies from sub-glacial to grounded ice-margin and glacio-marine facies.

REFERENCES (if any) ¹: **This is not exhaustive, as many are already in ASUD. These are the key resources for this definition card.**

- Ambrose, GJ, Flint, RB & Webb, AW 1981, 'Precambrian and Palaeozoic Geology of the Peake and Denison Ranges', Bulletin (50), Geological Survey of South Australia
- Coats RP & Preiss WV 1987, 'Stratigraphy of the Umberatana Group', IN: WV Preiss (compiler), 'The Adelaide Geosyncline – Later Proterozoic Stratigraphy, Sedimentation, Palaeontology and Tectonics', Bulletin (53), pp. 125–210, Geological Survey of South Australia
- Connor, CHH & Preiss, WV 2019, 'Cryogenian glaciomarine megaclasts of the MacDonald Corridor, Bimbowrie Conservation Park, Olary Region, South Australia', Australian Journal of Earth Sciences, vol. 67 (6), pp. 857-872. doi:10.1080/08120099.2018.1553206
- Cox, GM, Isakson, V, Hoffman, PF, Gernon, TM, Schmitz, MD, Shahin, S, Collins, AS, Preiss, WV, Blades, ML, Mitchell, RN & Nordsvan, A 2018, 'South Australian U-Pb zircon (CA-ID-TIMS) age supports globally synchronous Sturtian deglaciation', Precambrian Research, vol. 315, pp. 257-263. doi:10.1016/j.precamres.2018.07.007
- Forbes, BG & Cooper RS 1976, 'The Pualco Tillite of the Olary Region, South Australia', Quarterly Geological Notes, vol. 60, pp. 2–5, Geological Survey of South Australia
- Howchin, W 1920, 'Past Glacial Action in Australia', IN: Year Book (13), Australian Bureau of Statistics, Australia, pp. 1133-1146
- Keeman, J, Turner, S, Haines, PW, Belousova, E, Ireland, T, Brouwer, P, Foden, J & Wörner, G 2020, 'New UPb, Hf and O isotope constraints on the provenance of sediments from the Adelaide Rift Complex – Documenting the key Neoproterozoic to early Cambrian succession', Gondwana Research, vol. 83, pp. 248-278. doi:10.1016/j.gr.2020.02.005
- Link, PK 1977, 'Facies and palaeogeography of Late Precambrian Sturtian glacial sediments, Copley area, northern Flinders Ranges and in the Sturt Gorge near Adelaide, South Australia', Honours Thesis, University of Adelaide, <https://hdl.handle.net/2440/131122>
- Lloyd, JC, Blades, ML, Counts, JW, Collins, AS, Amos, KJ, Wade, BP, Hall, JW, Hore, S, Ball, AL, Shahin, S & Drabsch, M 2020, 'Neoproterozoic geochronology and provenance of the Adelaide Superbasin', Precambrian Research, vol. 350, p. 105849. doi:10.1016/j.precamres.2020.105849.
- [Pre-print] Lloyd, JC, Preiss WV, Collins, AS, Virgo, GM, Blades, ML, Gilbert, SE & Amos, KJ 2022a, 'Detrital zircon record of the Sturtian glaciation: Adelaide Superbasin', EarthArXiv (this preprint)
- [Pre-print] Lloyd, JC, Collins, AS, Blades, ML, Gilbert, SE & Amos, KJ 2022b, 'Late Tonian development of the Adelaide Superbasin', EarthArXiv, doi:10.31223/X5N63H
- Segnit, RW 1939, 'The Precambrian-Cambrian succession – The general and economic geology of these systems, in portions of South Australia', Bulletin (18), Geological Survey of South Australia
- Young, GM & Gostin, VA 1989, 'An exceptionally thick upper Proterozoic (Sturtian) glacial succession in the Mount Painter area, South Australia', Geological Society of America Bulletin, vol. 101 (6), ppp. 834-845. doi:10.1130/0016-7606(1989)101<0834:Aetups>2.3.Co;2

1561

(for subcommittee use only)

Definition approved by:

SA Stratigraphic Names Subcommittee

(delete where inapplicable)

Date:

(for registry use only)

Name first published by:

Definition by:

1562